

Ground-state energies, densities and momentum distributions in closed-shell nuclei calculated within a cluster expansion approach and realistic interactions

M. Alvioli and C. Ciofi degli Atti

*Department of Physics, University of Perugia and Istituto Nazionale di Fisica Nucleare,
Sezione di Perugia, Via A. Pascoli, I-06123, Perugia, Italy*

H. Morita

Sapporo Gakuin University, Bunkyo-dai 11, Ebetsu 069-8555, Hokkaido, Japan

(Dated: October 28, 2018)

Abstract

A linked cluster expansion suitable for the treatment of ground-state properties of complex nuclei, as well as of various particle-nucleus scattering processes, has been used to calculate the ground-state energy, density and momentum distribution of ^{16}O and ^{40}Ca using realistic interactions. First of all, a benchmark calculation for the ground-state energy has been performed using the truncated $V8'$ potential, and consisting in the comparison of our results with the ones obtained by the Fermi Hypernetted Chain approach, adopting in both cases the same mean field wave functions and the same correlation functions. The results exhibited a nice agreement between the two methods. Therefore, the approach has been applied to the calculation of the ground-state energy, density and momentum distributions of ^{16}O and ^{40}Ca using the full $V8'$ potential, finding again a satisfactory agreement with the results based on more advanced approaches where higher order cluster contributions are taken into account. It appears therefore that the cluster expansion approach can provide accurate approximations for various diagonal and non diagonal density matrices, so that it could be used for a reliable evaluation of nuclear effects in various medium and high energy scattering processes off nuclear targets. The developed approach can be readily generalized to the treatment of Glauber type final state interaction effects in inclusive, semi-inclusive and exclusive processes off nuclei at medium and high energies.

I. INTRODUCTION

The knowledge of the nuclear wave function, in particular its most interesting and unknown part, *viz* the correlated one, which is predicted by realistic many-body calculations to strongly deviate from a mean field description, is not only a prerequisite for understanding the details of bound hadronic systems, but is becoming at present a necessary condition for a correct description of medium and high energy scattering processes off nuclear targets; these, in fact, represent nowadays an efficient tool for the investigation of several high energy problems, e.g. color transparency, hadronization, the properties of dense hadronic matter, etc. which manifest themselves only in the nuclear medium. The necessity of an accurate treatment of the effects of the medium in high energy scattering process is becoming a relevant issue in hadronic physics. The problem is not trivial, for one has first to solve the many body problem and then has to find a way to describe scattering processes in terms of realistic many-body wave functions. The difficulty mainly arises because even if a reliable and manageable many-body description of the ground state is developed, the problem remains of the calculation of the final state. In the case of *few-body systems*, a consistent treatment of initial state correlations (ISC) and final state interaction (FSI) is nowadays possible at low energies by solving the Schrödinger equation for the bound and continuum states (see *e.g.*[1, 2, 3] and References therein quoted), but at high energies, when the number of partial waves sharply increases and nucleon excitations can occur, the Schrödinger approach becomes impractical and other methods have to be employed. Moreover, in the case of *complex nuclei*, additional difficulties arise due to the approximations which are still necessary to solve the many-body problem. As a matter of fact, in spite of the relevant progress made in recent years in the calculation of the properties of light nuclei (see *e.g.* [4, 5, 6, 7, 8]), much remains to be done, also in view that the results of very sophisticated calculations (*e.g.* the variational Monte Carlo ones [5]), show that the wave function which minimizes the expectation value of the Hamiltonian provides a very poor nuclear density; moreover, the structure of the best trial wave function is so complicated, that its use in the calculation of various processes at intermediate and high energies appears to be not easy task. It is for this reason that the evaluation of nuclear effects in medium and high energy scattering processes is usually carried out within simplified models of nuclear structure. As a matter of fact, ISC are often introduced by a procedure which has little to recommend

itself, namely the expectation value of the transition operator is evaluated with shell model (SM) uncorrelated wave functions and the initial two-body wave function describing the independent relative motion of two nucleons is replaced by a phenomenological correlated wave function. Recently, however, important progress has been made, in that ISC have been introduced from the beginning using correlated wave functions and cluster expansion techniques. Central Jastrow-type correlations have been often used to investigate the effects of ISC on various scattering processes off complex nuclei induced by medium energy leptons like, e.g. $A(e, e')X$ [10], $A(e, e'p)X$ [11] and $A(e, e'2N)X$ [12] processes. Calculations of inclusive electron scattering has also been performed using realistic many body wave functions and spectral functions within various approximations [13, 14], and non central correlations have been recently introduced in the calculation of $A(e, e'p)B$ and $A(e, e'2N)B$ [15, 16]. In spite of this progress, further work remains to be done to achieve a full consistent treatment of both ISC and FSI in intermediate and high energy scattering off complex nuclei. This would be particularly urgent, as far as various high energy phenomena are concerned, e.g. exclusive processes at high momentum transfer [17], inclusive [18] and semi inclusive [19] hadron production in Deep Inelastic Scattering, and others, which might also require a careful treatment of nuclear effects. As a matter of fact, a recent calculation [20] of the integrated nuclear transparency in the processes $^{16}O(e, e'p)X$ and $^{40}Ca(e, e'p)X$ performed within a cluster expansion approach, including realistic central and tensor correlations, shows that the results do depend both on the SM and ISC parameters, which have therefore to be fixed from firm criteria, e.g. from the calculation of the static properties of nuclei, like the ground-state energy and the density distribution.

For such a reason, we have undertaken the calculation of the basic ground-state properties (energies, densities and momentum distributions) of complex nuclei within a framework which can easily be generalized to the treatment of various scattering processes, keeping the basic features of ISC as predicted by the structure of realistic Nucleon-Nucleon (NN) interactions. Our approach is presented in detail in this paper, which is organized as follows: in Section II some basic ideas concerning the application of the cluster expansion techniques to the approximate solution of the nuclear many-body problem are recalled; the cluster expansion used in the calculations is described in Section III; the ground-state energy calculations for ^{16}O and ^{40}Ca are presented in Section IV, where the results a benchmark calculation aimed at a comparison of our results with the results obtained within the Fermion Hypernet-

ted Chain (FHNC) approach [7, 8, 9] is presented; the results of the calculations of the charge densities and momentum distributions are given in Sections V and VI, respectively; the diagrammatic representation of the latter quantities within the cluster-expansion approach are illustrated in Section VII; the Summary and Conclusions are presented in Section VIII.

Preliminary results of our calculations have been presented in Ref. [21, 22].

II. THE CORRELATED WAVE FUNCTIONS

It is well known that if nuclei are considered to be aggregates of point-like nucleons with the same properties and interactions as the free ones, and, moreover, all degrees of freedom but nucleonic ones are frozen, the nuclear many-body problem reduces to the search of the eigenvalues and eigenfunctions of the following Schrödinger equation [23]

$$\left[\sum_{i=1}^A \frac{\mathbf{p}_i^2}{2 M_N} + \hat{V}_{eff}(1, 2, \dots, A) \right] \psi_n(1, 2, \dots, A) = E_n \psi_n(1, 2, \dots, A) \quad (1)$$

where M_N is the nucleon mass and the effective interaction includes many-body interactions between the constituents, *i.e.*

$$\hat{V}_{eff}(1, 2, \dots, A) = \sum_{i < j} \hat{v}_2(i, j) + \sum_{i < j < k} \hat{v}_3(i, j, k) + \dots + v_A(1, 2, \dots, A). \quad (2)$$

Within the so called *standard model* of nuclei [24], which will be considered from now on, many-body interactions are disregarded and Eq. (1) is solved keeping only the two-body interaction $\hat{v}_2(i, j)$, whose form is determined from two-body bound and scattering data. We will consider therefore the following nuclear Hamiltonian:

$$\hat{H} = \hat{T} + \hat{V} = -\frac{\hbar^2}{2 M_N} \sum_{i=1}^A \nabla_i^2 + \sum_{i < j} \hat{v}_2(\mathbf{x}_i, \mathbf{x}_j), \quad (3)$$

where the vector \mathbf{x} denotes the set of nucleonic degrees of freedom, *i.e.* $\mathbf{x} \equiv (\mathbf{r}; \boldsymbol{\sigma}; \boldsymbol{\tau})$, with \mathbf{r} , $\boldsymbol{\sigma}$ and $\boldsymbol{\tau}$ denoting the spatial, spin and isospin coordinates, respectively. We will try to find the solution of the Schrödinger equation pertaining to the ground-state of the nucleus, *i.e.*:

$$\hat{H} \psi_o = E_o \psi_o \quad (4)$$

and to this end we will look for the ground-state wave function (WF) ψ_0 which minimizes the expectation value of the Hamiltonian

$$\langle \hat{H} \rangle = \frac{\langle \psi_o | \hat{H} | \psi_o \rangle}{\langle \psi_o | \psi_o \rangle} \geq E_o. \quad (5)$$

As trial WF we will use a correlated WF of the following form [26]

$$\psi_o(\mathbf{x}_1, \dots, \mathbf{x}_A) = \hat{F}(\mathbf{x}_1, \dots, \mathbf{x}_A) \phi_o(\mathbf{x}_1, \dots, \mathbf{x}_A), \quad (6)$$

where ϕ_o is a SM, mean-field WF describing the independent particle motion, and \hat{F} is a symmetrized *correlation operator*, which generates correlations into the mean field WF; the correct symmetry of the WF is guaranteed by ϕ_o .

As in any variational approach, the central problem here is to give an explicit form to the trial WF (Eq. (6)); whereas for ϕ_o any realistic SM WF can be considered a physically sound approximation, the choice of the form of the operator \hat{F} is not clear *a priori*. However one can be guided by the knowledge of the basic features of the force acting between the considered hadrons. Nowadays the nucleon-nucleon interaction can be cast in the following form ([25]):

$$\hat{V} = \sum_{n=1}^N v^{(n)}(r_{ij}) \hat{\mathcal{O}}_{ij}^{(n)}, \quad (7)$$

where $r_{ij} = |\mathbf{r}_i - \mathbf{r}_j|$ is the relative distance of nucleons i and j , and n , ranging up to $N = 18$, labels the state-dependent operator $\hat{\mathcal{O}}_{ij}^{(n)}$:

$$\hat{\mathcal{O}}_{ij}^{(n)} = [1, \boldsymbol{\sigma}_i \cdot \boldsymbol{\sigma}_j, \hat{S}_{ij}, (\mathbf{S} \cdot \mathbf{L})_{ij}, L^2, L^2 \boldsymbol{\sigma}_i \cdot \boldsymbol{\sigma}_j, (\mathbf{S} \cdot \mathbf{L})_{ij}^2, \dots] \otimes [1, \boldsymbol{\tau}_i \cdot \boldsymbol{\tau}_j] \quad (8)$$

Accordingly, the operator \hat{F} is written as

$$\hat{F}(\mathbf{x}_1, \mathbf{x}_2 \dots \mathbf{x}_A) = \hat{S} \prod_{i < j}^A \hat{f}(r_{ij}) \quad (9)$$

with

$$\hat{f}(r_{ij}) = \sum_{n=1}^N \hat{f}^{(n)}(r_{ij}) \quad \hat{f}^{(n)}(r_{ij}) = f^{(n)}(r_{ij}) \hat{\mathcal{O}}_{ij}^{(n)}. \quad (10)$$

The variational principle requires the full evaluation of Eq. (5) which, obviously, is no easy task due to the structure of ψ_0 . We will evaluate the expectation value of the Hamiltonian (5), using the cluster expansion techniques [26], adopting a specific cluster expansion to be described in the next sections.

III. THE CLUSTER EXPANSION

The evaluation of the expectation value of \hat{H} is object of intensive activity which in the last few years has produced considerable results: the approximate solution of the Schrödinger

equation by means of Monte Carlo methods, for example, has reached a great level of accuracy, and the ground-state properties of nuclei with $A = 16$ have been obtained with a full evaluation of Eq. (5) [4, 5]; exhaustive calculations have also been performed within the FHNC approximation [7, 8, 9]. Nevertheless, the level of complexity of these calculations often prevents the WF to be used with reasonable ease in other nuclear-related problems, such as nuclear reactions. Our goal is to present a more economical, but effective method for the calculation of the expectation value of any quantum mechanical operator $\hat{\mathcal{O}}$ in the many-body ground-state described by the WF ψ_o , *i.e.*:

$$\langle \hat{\mathcal{O}} \rangle = \frac{\langle \psi_o | \hat{\mathcal{O}} | \psi_o \rangle}{\langle \psi_o | \psi_o \rangle}; \quad (11)$$

with ψ_o having the structure of Eq. (6). In the present section we are going to introduce a cluster expansion technique in order to evaluate Eq. (11). To begin with, a generic operator $\hat{\mathcal{O}}$ in Eq. (11) will be considered in the following Section, while in the next Section, it will be specialized to the Hamiltonian and to the one- and two-body density operators.

Various types of cluster expansions have been used in the past to calculate the ground-state properties of nuclei (see e.g. [27, 28]); in these calculations, mainly aimed at investigating the convergence of the expansion, simple models of the NN interaction have been usually used. In this paper we use an expansion which has never been used previously to calculate ground-state properties of nuclei in terms of realistic interactions. The expansion we are going to use has been originally developed in Ref. [29] (see also [30] and [31]); the main feature of such an expansion is that it is linked and number conserving. The latter property means that the normalization of any observable is provided by the normalization of the mean field WF, *i.e.*, by the first term of the expansion: the contribution of all other terms to the normalization vanishes analytically order by order. The expansion, to be called the η -expansion, has been originally used to obtain the lowest order contribution to the diagonal one-body density (OBD) matrix, $\hat{\rho}^{(1)}(\mathbf{r}_1)$ [29], and to the one-body mixed density (OBMD) matrix, $\hat{\rho}^{(1)}(\mathbf{r}_1, \mathbf{r}'_1)$ [30], using central correlations only (*i.e.*, Eqs. (9) and (10) with $N = 1$). Subsequently [32], the lowest order expansion of the OBMD operator has been generalized to take into account also the non central spin-isospin and tensor-isospin correlations f^4 and f^6 in Eq. (10), which turned out to be the most relevant non central correlation functions in Nuclear Matter ([33]), as well as all correlations up to $N = 6$ [7]¹.

¹ The approximation which includes only the components $n = \{1, 4, 6\}$ is usually referred to as the f_3

During the last few years, lowest order expansions have also been applied, within the central correlation approximation, to the calculation of the two-body density matrix [34] and of various transition matrix elements appearing in inclusive, $A(e, e')X$, and exclusive, $A(e, e'p)B$ and $A(e, e'2N)B$, processes (see *e.g.* Refs. [10, 11, 12]). As already mentioned, the expansion has also been used, within the f_3 approximation, to calculate the nuclear transparency in the semi-inclusive process $A(e, e'p)X$ [20]. To our knowledge, the η -expansion has never been used to calculate the ground-state energy of complex nuclei with a realistic interaction. It is precisely the central aim of our work to present a detailed report of the results of the calculation of the ground-state energy, density and momentum distributions of complex nuclei using the η -expansion and realistic interactions.

Let us first of all recall the basic features of the expansion. Following the formal expression for ψ_o in 6, and taking the correlation operator \hat{F} as in 10, one writes

$$\begin{aligned}\hat{F}^2 &= \prod_{i < j} \hat{f}^2(r_{ij}) = \prod_{i < j} (1 + \hat{\eta}(r_{ij})) = \\ &= 1 + \sum_{i < j} \hat{\eta}_{ij} + \sum_{(ij) < (kl)} \hat{\eta}_{ij} \hat{\eta}_{kl} + \dots\end{aligned}\quad (12)$$

where

$$\hat{\eta}_{ij} \equiv \hat{f}_{ij}^2 - 1 \quad (13)$$

and $\langle |\eta|^2 \rangle$ will play the role of a *small* expansion parameter, in that its expectation value on the reference state ϕ_o is small. We use the notation $\eta_{ij} \equiv \eta(r_{ij})$. In what follows, when dealing with state-dependent operators, we have to bear in mind that they do not commute with each other; moreover, since the same operators appear both in the potential and in the WF, it is worth defining the following quantities:

- 1) $\langle A \rangle \equiv \langle \phi_o | A | \phi_o \rangle$, where A is an arbitrary quantity;
- 2) $\hat{\eta}_{ij} \hat{O} \equiv \hat{f}_{ij} \hat{O} \hat{f}_{ij} - \hat{O}$;
- 3) $\hat{\eta}_{ij} \hat{\eta}_{kl} \hat{O} \equiv \hat{f}_{ij} \hat{f}_{kl} \hat{O} \hat{f}_{ij} \hat{f}_{kl} - \hat{f}_{ij} \hat{O} \hat{f}_{ij} - \hat{f}_{kl} \hat{O} \hat{f}_{kl} + \hat{O}$;

and so on, where \hat{O} is the operator appearing in Eq. (11). Let us now perform the expansion of the expectation value (11). Keeping in mind the described recipes, the quantity $\hat{F}^\dagger \hat{F}$ is

approximation, whereas the approximation which includes all correlations up to $N = 6$ is referred to as the f_6 *approximation*.

expanded both in the numerator and the denominator and all terms containing the same number of functions $\eta_{ij} = \eta(ij)$ are collected, obtaining

$$\langle \hat{\mathcal{O}} \rangle = \mathcal{O}_0 + \mathcal{O}_1 + \mathcal{O}_2 + \dots + \mathcal{O}_n + \dots + \mathcal{O}_A, \quad (14)$$

At 2-nd order in η , one has, explicitly,

$$\mathcal{O}_0 \equiv \langle \hat{\mathcal{O}} \rangle, \quad (16a)$$

$$\mathcal{O}_1 = \left\langle \sum_{ij} \hat{\eta}_{ij} \hat{\mathcal{O}} \right\rangle - \mathcal{O}_0 \left\langle \sum_{ij} \hat{\eta}_{ij} \right\rangle, \quad (16b)$$

$$\mathcal{O}_2 = \left\langle \sum_{ij < kl} \hat{\eta}_{ij} \hat{\eta}_{kl} \hat{\mathcal{O}} \right\rangle - \left\langle \sum_{ij} \hat{\eta}_{ij} \hat{\mathcal{O}} \right\rangle \left\langle \sum_{ij} \hat{\eta}_{ij} \right\rangle + \quad (16c)$$

$$- \mathcal{O}_0 \left(\left\langle \sum_{ij < kl} \hat{\eta}_{ij} \hat{\eta}_{kl} \right\rangle - \left\langle \sum_{ij} \hat{\eta}_{ij} \right\rangle^2 \right); \quad (16d)$$

where the term of order n contains $\hat{\eta}(\hat{f})$ up to the n -th ($2n$ -th) power.

Analyzing the structure of Eqs. (16d) one realizes that there are terms which are due to the expansion of the denominator

$$\frac{1}{1-x} \simeq 1 + x + \dots, \quad (17)$$

e.g. the 2-nd term in Eq. (16b).

A nice feature of the η -expansion shows up at this point. Each of the terms in the residual formulæ presents some *linked* and *unlinked* contributions. What we mean by this is quite self-explaining when expressed in terms of standard Mayer diagrams [35], according to which in each linked term the involved $n < A$ particle coordinates are connected either by an f factor, or by Pauli correlations (see Section VII). It is precisely the expansion of the denominator which ensures that only linked terms contribute to the overall expectation value, all unlinked terms cancelling out amongst themselves. This feature turns out to be very convenient from a computational point of view, for it reduces the number of involved linked terms and allows one to obtain a very systematic and general procedure. Eventually it should be stressed that because of the non-commutative nature of the operators $\hat{\mathcal{O}}_{ij}^{(n)}$ involving at least one common particle index, sets of diagrams involving more than two particles appears in the expectation value of the Hamiltonian expression within the cluster expansion, already at first order.

IV. APPLICATION OF THE η -EXPANSION TO THE NUCLEI ^{16}O AND ^{40}Ca : GENERAL FORMULÆ AND A BENCHMARK CALCULATION WITH TRUNCATED $V8'$ AND $U14$ INTERACTIONS

A. General formulæ in terms of density distributions

Given the two-body interaction as in Eq. (7), the expectation value of the Hamiltonian can be written in the following way [35]:

$$E_o = -\frac{\hbar^2}{2M_N} \int d\mathbf{r}_1 \left[\nabla^2 \rho^{(1)}(\mathbf{r}_1, \mathbf{r}'_1) \right]_{\mathbf{r}_1=\mathbf{r}'_1} + \sum_n \int d\mathbf{r}_1 d\mathbf{r}_2 v^{(n)}(r_{12}) \rho_{(n)}^{(2)}(\mathbf{r}_1, \mathbf{r}_2), \quad (18)$$

where $\rho^{(1)}(\mathbf{r}_1, \mathbf{r}'_1)$ and $\rho^{(2)}(\mathbf{r}_1, \mathbf{r}_2)$ are the OBMD and the TBD matrices, respectively, which are defined as the expectation value of the operators

$$\hat{\rho}_1(\tilde{\mathbf{r}}_1, \tilde{\mathbf{r}}'_1) = \sum_i \delta(\mathbf{r}_i - \tilde{\mathbf{r}}_1) \delta(\mathbf{r}'_i - \tilde{\mathbf{r}}'_1) \prod_{j \neq i} \delta(\mathbf{r}_j - \mathbf{r}'_j) \quad (19)$$

and

$$\hat{\rho}_2(\tilde{\mathbf{r}}_1, \tilde{\mathbf{r}}_2) = \sum_{i < j} \delta(\mathbf{r}_i - \tilde{\mathbf{r}}_1) \delta(\mathbf{r}_j - \tilde{\mathbf{r}}_2), \quad (20)$$

i.e.

$$\rho^{(1)}(\mathbf{r}_1, \mathbf{r}'_1) = \langle \psi_o | \hat{\rho}_1(\mathbf{r}_1, \mathbf{r}'_1) | \psi'_o \rangle \quad (21)$$

$$\rho^{(2)}(\mathbf{r}_1, \mathbf{r}_2) = \langle \psi_o | \hat{\rho}_2(\mathbf{r}_1, \mathbf{r}_2) | \psi_o \rangle, \quad (22)$$

where

$$\psi_o \equiv \psi_o(\mathbf{x}_1, \dots, \mathbf{x}_A) \quad (23)$$

and

$$\psi'_o \equiv \psi_o(\mathbf{x}'_1, \dots, \mathbf{x}'_A) \quad (24)$$

and a summation over spin and isospin variables is implicit in Eqs. (21) and (22). The knowledge of the OBMD and TBD matrices allows one to calculate, besides the ground-state energy, other relevant quantities like *e.g.* the density distribution:

$$\rho(\mathbf{r}) = \rho^{(1)}(\mathbf{r}_1 = \mathbf{r}'_1 \equiv \mathbf{r}), \quad (25)$$

the mean square radius of the distribution:

$$\langle r^2 \rangle = \int d\mathbf{r} r^2 \rho(r) \quad (26)$$

and, eventually, the nucleon momentum distribution , *i.e.* the square of the WF in momentum space which, by definition, reads as follows:

$$n(\mathbf{k}) = \frac{1}{(2\pi)^3} \int d\mathbf{r}_1 d\mathbf{r}'_1 e^{i\mathbf{k}\cdot(\mathbf{r}_1 - \mathbf{r}'_1)} \rho(\mathbf{r}_1, \mathbf{r}'_1). \quad (27)$$

The normalization of the OBD, OBMD and TBD matrices are as follows

$$\int d\mathbf{r} \rho(\mathbf{r}) = A, \quad (28)$$

$$\int d\mathbf{r}'_1 \rho^{(1)}(\mathbf{r}_1, \mathbf{r}'_1) = \rho^{(1)}(\mathbf{r}_1) \quad (29)$$

$$\int d\mathbf{r}_1 d\mathbf{r}_2 \rho^{(2)}(\mathbf{r}_1, \mathbf{r}_2) = \frac{A(A-1)}{2}; \quad (30)$$

with the *sequential relation*

$$\int d\mathbf{r}_2 \rho^{(2)}(\mathbf{r}_1, \mathbf{r}_2) = \frac{A-1}{2} \rho^{(1)}(\mathbf{r}_1) \quad (31)$$

linking $\rho^{(2)}(\mathbf{r}_1, \mathbf{r}_2)$ to $\rho^{(1)}(\mathbf{r}_1)$. Accordingly, the normalization of the nucleon momentum distribution is

$$\int d\mathbf{k} n(\mathbf{k}) = A \quad (32)$$

It is useful at this moment to recall the form of $\rho(\mathbf{r}_1)$, $\rho^{(1)}(\mathbf{r}_1, \mathbf{r}'_1)$ and $\rho^{(2)}(\mathbf{r}_1, \mathbf{r}_2)$ predicted by the SM (or mean field) approximation. In this case one has $\psi_o = \phi_o = (A!)^{-1/2} \det\{\varphi_{\alpha_i}(\mathbf{x}_j)\}$, with the single particle (s.p.) orbitals given by $\varphi_{\alpha}(\mathbf{x}) = \varphi_a(\mathbf{r}) \chi_{\sigma}^{1/2} \xi_{\tau}^{1/2}$, where $\alpha \equiv \{a; \sigma; \tau\} = \{n, l, m; \sigma; \tau\}$. For closed shell nuclei one obtains:

$$\rho_{SM}^{(1)}(\mathbf{r}_1) = \sum_{\alpha} |\varphi_{\alpha}(\mathbf{x}_1)|^2 = 4 \rho_o(\mathbf{r}_1) \quad (33)$$

and

$$\rho_{SM}^{(1)}(\mathbf{r}_1, \mathbf{r}'_1) = \sum_{\alpha} \varphi_{\alpha}^*(\mathbf{x}_1) \varphi_{\alpha}(\mathbf{x}'_1) = 4 \rho_o^{(1)}(\mathbf{r}_1, \mathbf{r}'_1) \quad (34)$$

where the sum over α runs over the occupied SM states below the Fermi level, and

$$\rho_o(\mathbf{r}_1) = \sum_a |\varphi_a(\mathbf{r}_1)|^2 \quad (35)$$

and

$$\rho_o^{(1)}(\mathbf{r}_1, \mathbf{r}'_1) = \sum_a \varphi_a^*(\mathbf{r}_1) \varphi_a(\mathbf{r}'_1). \quad (36)$$

For the TBD matrix one obtains

$$\begin{aligned}\rho_{SM}^{(2)}(\mathbf{r}_1, \mathbf{r}_2) &= \frac{1}{2} \sum_{\alpha\beta} \left(\varphi_{\alpha}^{\star}(\mathbf{x}_1) \varphi_{\beta}^{\star}(\mathbf{x}_2) \varphi_{\alpha}(\mathbf{x}_1) \varphi_{\beta}(\mathbf{x}_2) - \varphi_{\alpha}^{\star}(\mathbf{x}_1) \varphi_{\beta}^{\star}(\mathbf{x}_2) \varphi_{\beta}(\mathbf{x}_1) \varphi_{\alpha}(\mathbf{x}_2) \right) \\ &= \frac{1}{2} 4 \left(4 \rho_o(\mathbf{r}_1) \rho_o(\mathbf{r}_2) - \rho_o^{(1)}(\mathbf{r}_1, \mathbf{r}_2) \rho_o^{(1)}(\mathbf{r}_2, \mathbf{r}_1) \right),\end{aligned}\quad (37)$$

where $\rho_o(\mathbf{r}_i) = \rho_o^{(1)}(\mathbf{r}_i, \mathbf{r}_i)$. When Eq. (21) is evaluated with the correlated wave functions (6) within the f_6 approximation, at first order of the η -expansion the following expression is obtained:

$$\rho^{(1)}(\mathbf{r}_1, \mathbf{r}'_1) = \rho_{SM}^{(1)}(\mathbf{r}_1, \mathbf{r}'_1) + \rho_H^{(1)}(\mathbf{r}_1, \mathbf{r}'_1) + \rho_S^{(1)}(\mathbf{r}_1, \mathbf{r}'_1), \quad (38)$$

with

$$\begin{aligned}\rho_H^{(1)}(\mathbf{r}_1, \mathbf{r}'_1) \\ = \int d\mathbf{r}_2 \left[H_D(r_{12}, r_{1'2}) \rho_o^{(1)}(\mathbf{r}_1, \mathbf{r}'_1) \rho_o(\mathbf{r}_2) - H_E(r_{12}, r_{1'2}) \rho_o^{(1)}(\mathbf{r}_1, \mathbf{r}_2) \rho_o^{(1)}(\mathbf{r}_2, \mathbf{r}'_1) \right]\end{aligned}\quad (39)$$

$$\begin{aligned}\rho_S^{(1)}(\mathbf{r}_1, \mathbf{r}'_1) \\ = - \int d\mathbf{r}_2 d\mathbf{r}_3 \rho_o^{(1)}(\mathbf{r}_1, \mathbf{r}_2) \left[H_D(r_{23}) \rho_o^{(1)}(\mathbf{r}_2, \mathbf{r}'_1) \rho_o(\mathbf{r}_3) - H_E(r_{23}) \rho_o^{(1)}(\mathbf{r}_2, \mathbf{r}_3) \rho_o^{(1)}(\mathbf{r}_3, \mathbf{r}'_1) \right]\end{aligned}\quad (40)$$

where $r_{ij} = |\mathbf{r}_i - \mathbf{r}_j|$. The subscripts H and S , whose meaning will be explained in Section VII, stand for *hole* and *spectator*, respectively, and

$$H^{D(E)}(r_{ij}, r_{kl}) = \sum_{p,q=1}^6 f^{(p)}(r_{ij}) f^{(q)}(r_{kl}) C_{D(E)}^{(p,q)}(r_{ij}, r_{kl}) - C_{D(E)}^{(1,1)}(r_{ij}, r_{kl}). \quad (41)$$

Here the subscripts D and E stand for *direct* and *exchange*, respectively, and the coefficients $C_D^{(p,q)}(r_{ij}, r_{kl})$, $C_E^{(p,q)}(r_{ij}, r_{kl})$, whose explicit expressions are given in Appendix C, result from the *spin* and *isospin* summation, and their explicit dependence upon the coordinates originates from the tensor operator. As for the correlated TBD matrix, this can be obtained by multiplying the TBD operator in Eq. (20) by the operators $\hat{\mathcal{O}}_{ij}^{(n)}$ of Eq. (8); the resulting TBD matrix, corresponding to the operator $\hat{\mathcal{O}}_{ij}^{(n)}$ reads as follows:

$$\rho_{(n)}^{(2)}(\mathbf{r}_1, \mathbf{r}_2) = \rho_{(n)}^{(A)}(\mathbf{r}_1, \mathbf{r}_2) + \rho_{(n)}^{(B)}(\mathbf{r}_1, \mathbf{r}_2) + \rho_{(n)}^{(C)}(\mathbf{r}_1, \mathbf{r}_2) + \rho_{(n)}^{(D)}(\mathbf{r}_1, \mathbf{r}_2) \quad (42)$$

$$\begin{aligned}\rho_{(n)}^{(A)}(\mathbf{r}_1, \mathbf{r}_2) &= \frac{1}{A(A-1)} \sum_{p,q=1}^6 f_{12}^{(p)} f_{12}^{(q)} \sum_{r,s=1}^6 \left((K_{(p,q)}^{(r)} K_{(r,n)}^{(s)} A_D^{(s)} - A_D^{(n)}) \rho_o(\mathbf{r}_1) \rho_o(\mathbf{r}_2) \right. \\ &\quad \left. - (K_{(p,q)}^{(r)} K_{(r,n)}^{(s)} A_E^{(s)} - A_E^{(n)}) \rho_o(\mathbf{r}_1, \mathbf{r}_2) \rho_o(\mathbf{r}_2, \mathbf{r}_1) \right)\end{aligned}\quad (43)$$

$$\begin{aligned} \rho_{(n)}^{(B)}(\mathbf{r}_1, \mathbf{r}_2) = & \frac{1}{A(A-1)} \int d\mathbf{r}_3 \sum_{\mathcal{P}} \left(\sum_{p,q=1}^6 f_{13}^{(p)} f_{13}^{(q)} B_{(n),\mathcal{P}}^{(p,q)} - B_{(n),\mathcal{P}}^{1,1} \right) \times \\ & \times \rho_o(\mathbf{r}_1, \mathbf{r}_{\mathcal{P}\{1\}}) \rho_o(\mathbf{r}_2, \mathbf{r}_{\mathcal{P}\{2\}}) \rho_o(\mathbf{r}_3, \mathbf{r}_{\mathcal{P}\{3\}}) \end{aligned} \quad (44)$$

$$\begin{aligned} \rho_{(n)}^{(C)}(\mathbf{r}_1, \mathbf{r}_2) = & \frac{1}{A(A-1)} \int d\mathbf{r}_3 \sum_{\mathcal{P}} \left(\sum_{p,q=1}^6 f_{23}^{(p)} f_{23}^{(q)} C_{(n),\mathcal{P}}^{(p,q)} - C_{(n),\mathcal{P}}^{1,1} \right) \times \\ & \times \rho_o(\mathbf{r}_1, \mathbf{r}_{\mathcal{P}\{1\}}) \rho_o(\mathbf{r}_2, \mathbf{r}_{\mathcal{P}\{2\}}) \rho_o(\mathbf{r}_3, \mathbf{r}_{\mathcal{P}\{3\}}) \end{aligned} \quad (45)$$

$$\begin{aligned} \rho_{(n)}^{(D)}(\mathbf{r}_1, \mathbf{r}_2) = & \frac{1}{A(A-1)} \frac{1}{2} \int d\mathbf{r}_3 d\mathbf{r}_4 \sum_{\mathcal{P}} \left(\sum_{p,q=1}^6 f_{34}^{(p)} f_{34}^{(q)} \sum_{r=1}^6 K_{(p,q)}^{(r)} D_{(n),\mathcal{P}}^{(r)} - D_{(n),\mathcal{P}}^{(1)} \right) \times \\ & \times \rho_o(\mathbf{r}_1, \mathbf{r}_{\mathcal{P}\{1\}}) \rho_o(\mathbf{r}_2, \mathbf{r}_{\mathcal{P}\{2\}}) \rho_o(\mathbf{r}_3, \mathbf{r}_{\mathcal{P}\{3\}}) \rho_o(\mathbf{r}_4, \mathbf{r}_{\mathcal{P}\{4\}}) \end{aligned} \quad (46)$$

This expression deserves a few explanations; $A_{D(E)}^{(n)}$, $B_{(n),\mathcal{P}}^{(p,q)}$, $C_{(n),\mathcal{P}}^{(p,q)}$ and $D_{(n),\mathcal{P}}^{(r)}$ are the result of the spin-isospin summations and they are in general function of the coordinates; the remaining summations over the spatial quantum numbers are then expressed in terms of combinations of *OBMD* matrices (see Appendix C); the subindex \mathcal{P} in these factors stands for all possible permutations of the states but the *unlinked* one and the sub-indexes $\mathcal{P}\{i\}$ means the corresponding index resulting from the particular permutations; finally, the matrices $K_{(p,q)}^{(r)}$ are proper *numerical* combination of the spin-isospin operators $\hat{\mathcal{O}}_{ij}^{(n)}$, and are defined by the following relation

$$\hat{\mathcal{O}}_{(m,n)}^{(p)} \hat{\mathcal{O}}_{(m,n)}^{(q)} = \sum_{r=1}^6 K_{(p,q)}^{(r)} \hat{\mathcal{O}}_{(m,n)}^{(r)} \quad (47)$$

Note that even if we are dealing with two-body correlations and interactions we end up with three- and four-body operators, due to the fact that, *e.g.* terms like $\hat{\mathcal{O}}_{(1,2)} \hat{\mathcal{O}}_{(1,3)}$, cannot be further reduced. Thus, the first order η -expansion for the energy gets contributions from up to four-body clusters.

From the definition of the nucleon momentum distribution, *i.e.* Eq.(27), we can obtain the expectation value of the kinetic energy operator as follows:

$$\langle \hat{T} \rangle = \frac{\hbar^2}{2 M_N} \int d\mathbf{k} k^2 n(\mathbf{k}) . \quad (48)$$

and Eq. (18), finally becomes

$$E_o = \frac{\hbar^2}{2 M_N} \int d\mathbf{k} k^2 n(\mathbf{k}) + \sum_n \int d\mathbf{r}_1 d\mathbf{r}_2 v^{(n)}(r_{12}) \rho_{(n)}^{(2)}(\mathbf{r}_1, \mathbf{r}_2) , \quad (49)$$

with $\rho_{(n)}^{(2)}(\mathbf{r}_1, \mathbf{r}_2)$ given by Eq. (42). This is the final expression which has been used to calculate the ground-state energy by the following procedure: we have calculated at the same order both $n(k)$ and $\rho_n^{(2)}$, then by placing them in Eq. (49) and performing the summation over n the ground state energy E_0 is obtained. Calculations have been performed with a given, fixed form for the correlation functions, and considering as variational parameters, the parameters of the mean field wave functions. To begin with, in the next Section the results of a benchmark calculation aimed at investigating the convergence of the expansion will be presented.

B. A benchmark calculation for ^{16}O and ^{40}Ca : comparison between the η -expansion and the Fermion-Hyper-Netted-Chain / Single Operator Chain (FHNC/SOC) approach with truncated $V8'$ and $U14$ interactions

In order to investigate the convergence of the η -expansion, we have performed a benchmark calculation consisting in a comparison of Eq. (49) with the energy predicted by the FHNC/SOC approach. Namely, we have calculated the ground-state properties of ^{16}O and ^{40}Ca using the first six components of the $V8'$ [36] and $U14$ [38] interactions, respectively (these model interactions are usually referred to as the *truncated* $V8'$ and $U14$ interactions). The results we have obtained are compared with the results obtained with FHNC/SOC using the same interaction, the same mean field WF's, and the same correlation functions. The six correlation functions used in the calculation for ^{16}O , corresponding to the $V8'$ interaction, are shown in Fig. 1, and the results of the energy calculation are presented in Tables I and II. It can be seen that the cluster expansion results are very similar to the ones provided by the FHNC/SOC method; particularly worth being mentioned is the almost identical value of the mean kinetic energy, which means that the nucleon momentum distributions predicted by the two methods are very similar. The results of the calculation for ^{40}Ca , corresponding to the truncated $U14$ interaction [38] and to the mean field and correlation functions shown in Fig. 2, are presented in Table III where they are compared with the results of the FHNC/SOC approach of Ref. [8]. Being the mean field wave functions and correlation functions the same in the two calculations, any difference between our results and those of Ref. [8] has to be ascribed, as in the case of ^{16}O , to the contributions that are left out in the cluster expansion. It can be seen that the difference between the two approaches is larger

in ^{40}Ca than in the ^{16}O case, the largest difference arising from the spin-isospin interaction, which as a matter of fact is of longer range in ^{40}Ca (cf. Fig. 2).

To sum up, it seems that the convergence of the η -expansion for the ground-state energy is a satisfactory one.

V. APPLICATION OF THE η -EXPANSION TO THE NUCLEI ^{16}O AND ^{40}Ca : THE GROUND-STATE ENERGY, RADIUS AND DENSITIES WITH THE FULL $V8'$ INTERACTION

In Ref. [7], using the full $V8'$ interaction which includes the spin-orbit contributions v_7 and v_8 , several ground-state properties of ^{16}O and ^{40}Ca have been calculated within the FHNC/SOC approach, namely the ground state energy and the density and momentum distributions. For this reason, we have also calculated the ground-state properties of ^{16}O and ^{40}Ca using the η -expansion and the correlation functions of Ref. [7] which are shown in Fig. 3 and 4. The FHNC/SOC calculation of Ref. [7] was performed within the f_6 approximation. We have also used such an approximation but, unlike Ref. [7], we have disregarded the v_7 and v_8 components of the $V8'$ interaction. For such a reason a direct comparison of the results for the potential energy is not possible, whereas a comparison of the average kinetic energy is fully meaningful. The results of the comparison are presented in Tables V and VI for ^{16}O , and VII and VIII for ^{40}Ca . The most striking feature of the correlation functions obtained in Ref. [7] is the long tail of the tensor-isospin correlation function f^6 , which is expected to affect the convergence of the cluster expansion. As a matter of fact, it can be seen that whereas the difference in $\langle T \rangle$ are of the same order as in the benchmark calculation, for $\langle V \rangle$ the situation is not as good as for $\langle T \rangle$. The reason should probably be ascribed to the long tail in f^6 , and the spin-orbit term in the interaction which is dropped in the present calculation. As far as the latter is concerned, we have estimated the effect of the inclusion of the angular momentum dependent terms, by using the nuclear matter results of Ref.[7], and the discrepancy for the nuclear matter case seems to be consistent with the discrepancy we found.

The results we have obtained deserve the following comments

- i) We have compared our results obtained with the truncated $V8'$ and the f_6 approximation but using the full $V8'$ potential which includes the v_7 and v_8 components. Since in

both calculations the same mean field WF and correlations functions have been used, the differences between the two results have to be ascribed to the terms left out in the cluster expansion. Our estimate of the contribution of the v_7 and v_8 , based on nuclear matter results, shows that this seems indeed to be the case;

- ii) the average kinetic energy obtained in [7] agrees with the one obtained by our approach; we will indeed show that the momentum distribution, from which the kinetic energy is obtained, (see Eq. (48)), is in very good agreement with the one obtained in [7]. Some discrepancies are still present as far as the potential energy is concerned, but obtaining a full agreement between the lowest order cluster expansion and the FHNC/SOC approaches is illusory.
- iii) the overall value of the ground-state energy obtained in this section is reasonably closer to the experimental one ($\simeq 8$ MeV per nucleon) and it appears that the η -expansion provides a reasonable WF as far as the expectation value of the Hamiltonian is concerned.

By letting $\mathbf{r}_1 = \mathbf{r}'_1 \equiv \mathbf{r}$ in Eq. (38), the matter density at first order of the η -expansion, is obtained, *i.e.*

$$\begin{aligned} \rho(\mathbf{r}) = & 4\rho_o(\mathbf{r}) \\ & + \int d\mathbf{r}_2 \left[H_D(r_{12}) \rho_o(\mathbf{r}) \rho_o(\mathbf{r}_2) - H_E(r_{12}) \rho_o^{(1)}(\mathbf{r}, \mathbf{r}_2) \rho_o^{(1)}(\mathbf{r}_2, \mathbf{r}) \right] \\ & - \int d\mathbf{r}_2 d\mathbf{r}_3 \rho_o^{(1)}(\mathbf{r}, \mathbf{r}_2) \left[H_D(r_{23}) \rho_o(\mathbf{r}_2, \mathbf{r}) \rho_o(\mathbf{r}_3) - H_E(r_{23}) \rho_o^{(1)}(\mathbf{r}_2, \mathbf{r}_3) \rho_o^{(1)}(\mathbf{r}_3, \mathbf{r}) \right]. \end{aligned} \quad (50)$$

The charge density is obtained by convoluting $\rho(\mathbf{r})$ with the charge density of the proton and by correcting for the center-of-mass motion (see *e.g.* [39]). Using the mean field WF and the correlation functions obtained from the ground-state energy calculation with the full $V8'$ interaction (cf. Figs. 3 and 4 and Tables V-VIII), the densities shown in Figs. 5 and 6 for ^{16}O and for ^{40}Ca , respectively, are obtained. The results presented in Fig. 5 and Fig. 6 clearly show that the charge density calculated within the first order η -expansion agrees very well with the results obtained in [7] within the FHNC/SOC approach, which indicates a very good convergence of the η -expansion as far as the density is concerned.

It should however be pointed out, that, as first found in [7], the density calculated with mean field WF which minimizes the ground-state energy, strongly disagree with the experimental density. To cure such a problem, following Ref. [7], we have recalculated the density

varying the mean field parameters to obtain an agreement with the experimental density. We take advantage of the fact that, as shown in Fig. 7, the energy minimum calculated within the η -expansion is a rather shallow one. The results are shown in Figs. 8 and 9, and the comparison with the results of Ref. [7] demonstrate once again the good convergence of the η -expansion.

The six different two-body densities distributions (Eqs. (42)-(46)) corresponding to the first six correlation operators, are shown in Fig. 10 for ^{16}O (*top*) and ^{40}Ca (*bottom*): each of these densities couples with the corresponding component of the realistic potential to give the potential energy expectation value. Note that the quantities shown in Fig. 10 are integrated over the center of mass variable , i.e.

$$\rho_{(n)}^{(2)}(r) = 4\pi \int d\mathbf{R} \rho_{(n)}^{(2)} \left(\mathbf{R} = \frac{1}{2}(\mathbf{r}_1 + \mathbf{r}_2), r \equiv |\mathbf{r}| = |\mathbf{r}_1 - \mathbf{r}_2| \right). \quad (51)$$

VI. APPLICATION OF THE η -EXPANSION TO THE NUCLEI ^{16}O AND ^{40}Ca : THE NUCLEON MOMENTUM DISTRIBUTIONS

Using the correlation functions shown in Figs. 3 and 4, and the mean field WF's corresponding to the best densities shown in Figs. 8 and 9 , we have calculated the momentum distributions given by Eq. (27), with the OBMD matrix $\rho^{(1)}(\mathbf{r}_1, \mathbf{r}'_1)$ given by Eq. (38). The results, obtained at first order in η (the convergence will be discussed later on), are presented in Figs. 11, 12, 13 and 14. In Figs. 11 and 12, our results are compared with the the results obtained in Ref. [7], where the same interaction and the same correlation functions have been used, and in case of ^{16}O , also with the results of Ref. [5] where the AV14 interaction [36] and the Variational Monte Carlo approach have been used. These comparisons show that:

1. our results nicely agree with the ones of Refs. [7] and [5];
2. short range central correlations do not produce enough high momentum components, although they appreciably affect the momentum distributions at $k \geq 2 \text{ fm}^{-1}$;the inclusion of the tensor operators greatly enhances the high-momentum tail of the distribution in the region $k > 2 \text{ fm}^{-1}$.

3. the largest effect from non central correlations comes from tensor (\hat{S}_{ij}) and tensor-isospin ($\hat{S}_{ij} \boldsymbol{\tau}_i \cdot \boldsymbol{\tau}_j$) correlations ($n = 4$ and $n = 6$ in Eq. (8)), the other components playing a minor role; thus, as shown in Fig. 13, the f_3 approximation appears to be a rather good one for the calculation of the momentum distributions;
- iv) the satisfactory agreement of our results with the ones of Refs. [7] and [5] shows that the convergence of the η -expansion for $\rho(\mathbf{r}, \mathbf{r}')$ is a very good one. As a matter of fact, we have explicitly evaluated the next order cluster contribution for ^{16}O ; the results, reported in Fig. 14 using the f_3 approximation for the correlations functions, show a very good convergence indeed.

We would like to stress that the good convergence of the momentum distributions is a proof of the good convergence of $\langle T \rangle$.

VII. EFFECTS OF CORRELATIONS ON THE CHARGE DENSITY AND MOMENTUM DISTRIBUTIONS: THE DIAGRAMMATIC DESCRIPTION

Within any body approach based upon the correlated wave function (6), the interaction (7) and the cluster expansion technique, any quantity can be described by a diagrammatic representation, which provides a meaningful definition of correlations and the extent to which they affect the given quantity. In particular, the density and the momentum distributions are associated to diagrams according to the following rules (see e.g. Ref. [29]):

1. an open dot with the index i denotes the coordinate \mathbf{r}_i ;
2. a full dot with index i stands for integration over \mathbf{r}_i ;
3. an oriented line joining two dots with indexes i and j denotes $\rho_o^{(1)}(\mathbf{r}_i, \mathbf{r}_j)$;
4. a line beginning from and ending in a dot with index i denotes $\rho_o(\mathbf{r}_i)$;
5. a dashed line joining two full dots with indexes i and j denotes $H^{D(E)}(\mathbf{r}_{ij})$;
6. two dashed lines joining the open dots with index i and j with the full dot denotes $H^{D(E)}(\mathbf{r}_{ij}, \mathbf{r}_{i'j})$.

The diagrammatic representations of the diagonal (Eq. (50)) and non diagonal (Eq. (38)) one body density matrices are shown in Figs. 15 and 16 respectively. The meaning of *hole* (H) and *spectator* (S) contributions introduced in Section IV A (cf. Eqns. (39) and (40)) becomes now clear: the first, represented by diagrams 15b (16b) describes the process in which particle "1" is correlated with particle "2", whereas the second one, represented by diagrams 15c (16c), describes the process in which dynamical correlations are acting between particles "2" and "3". In Figs. 17 and 18 we show the effect of the hole and spectator contributions on the charge density and momentum distributions, respectively. It can be seen that the effects on the two quantities are very different: as far as the density is concerned, $\Delta\rho^H$ and $\Delta\rho^S$ are almost of the same value, and of opposite sign, with a small net effect; as for the momentum distribution, the spectator contribution only affects the SM distribution by an almost constant factor of 0.8, whereas the hole contribution creates the large amount of high momentum components. The spectator contribution leads to a renormalization of the mean field orbitals and to a decrease of the occupation number for states below the Fermi level, whereas the hole contribution is responsible for the high momentum components. This explains and qualitatively justifies the parameterized $n(k)$ of Ref. [41] in the form $n(k) = n_o(k) + n_1(k)$. It is clear, that the amount of hole and spectator correlations also depends upon the amount of the mean field contributions; calculations show however that the latter, even if obtained within the most sophisticated mean field approaches, cannot never provide, e.g. the amount of high momentum components generated by the hole contribution, so that the high momentum part of $n(k)$ is practically due only to (hole) correlations. Other quantities which are very sensitive to hole correlations will be discussed elsewhere [42].

VIII. SUMMARY AND CONCLUSIONS

In this paper we have addressed the problem of developing a method which could be used to calculate scattering processes at medium and high energies within a realistic and parameter-free description of nuclear structure. The η -expansion seems to satisfy such a requirement: as a matter of fact, it can be used within the following strategy: *i*) the values of the parameters pertaining to the correlation functions and the mean field wave functions, can be obtained from the calculation of the ground-state energy, radius and density of the

nucleus, to a given order of the expansion; *ii)* using these parameters, any scattering process can be evaluated at the same order of the cluster expansion. The method therefore appears to be a very effective, transparent and parameter-free one. It should however be pointed out that, as any other many body approach, our cluster expansion approach may suffer from the well known convergence problem, so that the role played by the disregarded higher order terms has to be estimated. This is precisely what has been done in the present paper, adopting the following procedure: *i)* our lowest order results have been compared with the ones obtained within more complete approaches, like *e.g.* the FHNC and VMC methods, and *ii)* a direct calculation of the higher order terms of the momentum distribution $n(\mathbf{k})$ has been performed. It turned out that the value of the ground-state energy calculated within the first order η -expansion reasonably agrees with the one obtained within the FHNC/SOC approach. The agreement is very good as far as the average kinetic energy is concerned, whereas differences occur in some of the potential energy contributions, as it should have been expected due to the complex spatial dependence of some of the components of the nucleon-nucleon interaction. Nonetheless, using the same correlation functions as in the FHNC/SOC calculation, we obtain a reasonable minimum value of the energy, with mean field WF very near to the ones of the FHNC/SOC approach. Furthermore, our results for the charge density and momentum distributions shows a very good agreement with the results obtained within the FHNC/SOC approach and even with the VMC approach, and the direct calculation of the higher order terms in the expansion of the momentum distributions shows a very good convergence of the η -expansion up to very high values of the momentum.

To sum up, we have shown that, using realistic models of the nucleon-nucleon interaction, a proper approach based on cluster expansion techniques can produce reliable approximations for those diagonal and non diagonal density matrices which appear in various medium and high energy scattering processes off nuclei, so that the role of nuclear effects in these processes can be reliably estimated without using free parameters to be fitted to the data. The approach has already been extended to the treatment of the final state interaction effects in $A(e, e'p)X$ processes at medium energies within the eikonal-Glauber multiple scattering theory, and to the calculation of nuclear and color transparencies effects. Preliminary results [22] are very encouraging. Calculations of other types of high energy scattering processes (*e.g.* the total nucleon-Nucleus cross section) are in progress and will be reported elsewhere [42].

IX. ACKNOWLEDGMENTS

We are grateful to Giampaolo Co' for providing the FHNC results used in the benchmark calculation and to Adelchi Fabrocini who supplied us with the correlation functions corresponding to the $V8'$ interaction. One of us (CcdA) would like to thank Rafael Guardiola for enlightening discussions.

APPENDIX A: MEAN FIELD WAVE FUNCTIONS

The mean field wave functions have the general form:

$$\psi_{nlm}(\mathbf{r}) = R_{nl}(r) Y_{lm}(\theta, \varphi) \quad (\text{A1})$$

with $R_{nl}(r)$ the radial part and $Y_{lm}(\theta, \varphi)$ the spherical harmonics. We have used harmonic oscillator and Saxon-Woods wells to generate the radial part; in the harmonic oscillator case, we have

$$R_{nl}(r) = e^{-x/2} x^{l/2} U_{nl} X_{nl}^{1/2} \Psi \quad (\text{A2})$$

with $x = r^2/a^2$, a is the HO parameter and

$$U_{nl} = \sum_{k=1}^n \frac{(-1)^k x^k n! 2^k (2l+1)!!}{(n-k)! k! (2l+2k+1)!!}, \quad (\text{A3})$$

$$X_{nl} = \frac{2^{l-n+2} (2l+2n+1)!!}{(2l+1)!!^2 n! \pi^{1/2} a^3}; \quad (\text{A4})$$

whereas, in the Saxon-Woods case, the radial part is the solution of the radial Schrödinger equation with one-body potential of the following form

$$V_{SW}(r) = - \frac{V_o}{1 + e^{-(r-R_o)/a_o}}. \quad (\text{A5})$$

APPENDIX B: PARAMETERIZATION OF THE CORRELATION FUNCTIONS FOR ^{16}O AND ^{40}Ca

The correlation functions $f^{(n)}(r)$ for ^{16}O and ^{40}Ca , shown in Figs. 3 and 4, respectively, can be conveniently parameterized in the following way:

$$f^{(n)}(r) = \sum_{i=1}^6 A_i^{(n)} e^{-B_i^{(n)} r^i} \quad n = 1, \dots, 5 \quad (\text{B2a})$$

$$f^{(6)}(r) = A_2^{(6)} r^2 e^{-B_1^{(6)} r} + \sum_{i=2}^6 A_i^{(6)} r^{i-1} e^{-B_i^{(6)} r^i} \quad (\text{B2b})$$

where the parameters $A_i^{(n)}$ and $B_i^{(n)}$ are given in Table IX for ^{16}O and in Table X for ^{40}Ca .

APPENDIX C: THE COEFFICIENTS OF THE ONE BODY NON DIAGONAL DENSITY MATRIX RESULTING FROM THE SPIN-ISOSPIN SUMMATION

The coefficients appearing in Eq. (41) for the OBMD are defined as

$$\begin{aligned} C_D^{(p,q)}(r_{12}, r_{1'2}) &= \sum_{\sigma_1, \sigma_2, \tau_1, \tau_2} \langle \sigma_1 \tau_1 \sigma_2 \tau_2 | \hat{O}_{12}^{(p)} \hat{O}_{1'2}^{(q)} | \sigma_1 \tau_1 \sigma_2 \tau_2 \rangle, \\ C_E^{(p,q)}(r_{12}, r_{1'2}) &= \sum_{\sigma_1, \sigma_2, \tau_1, \tau_2} \langle \sigma_1 \tau_1 \sigma_2 \tau_2 | \hat{O}_{12}^{(p)} \hat{O}_{1'2}^{(q)} | \sigma_2 \tau_2 \sigma_1 \tau_1 \rangle \end{aligned} \quad (C1)$$

and can be calculated analytically; their explicit values are summarized in Table XI.

The coefficients appearing in the definition of the TBD are more involved and can only be written in terms of the spin-isospin states upon which they have to be calculated:

$$A_D^{(n=1,6)} = \{16, 0, 0, 0, 0, 0\}; \quad A_E^{(n=1,6)} = \{4, 12, 12, 36, 0, 0\}; \quad (C2)$$

$$B_{(n),\mathcal{P}}^{(p,q)} = \sum_{\sigma, \tau} \langle \sigma_1 \tau_1, \sigma_2 \tau_2, \sigma_3 \tau_3 | \hat{O}_{13}^{(p)} \hat{O}_{12}^{(n)} \hat{O}_{13}^{(q)} | \sigma_1 \tau_1, \sigma_2 \tau_2, \sigma_3 \tau_3 \rangle_{\mathcal{P}} \quad (C3)$$

$$C_{(n),\mathcal{P}}^{(p,q)} = \sum_{\sigma, \tau} \langle \sigma_1 \tau_1, \sigma_2 \tau_2, \sigma_3 \tau_3 | \hat{O}_{23}^{(p)} \hat{O}_{12}^{(n)} \hat{O}_{23}^{(q)} | (\sigma_1 \tau_1, \sigma_2 \tau_2, \sigma_3 \tau_3) \rangle_{\mathcal{P}} \quad (C4)$$

$$D_{(n),\mathcal{P}}^{(q)} = \sum_{\sigma, \tau} \langle \sigma_1 \tau_1, \sigma_2 \tau_2, \sigma_3 \tau_3, \sigma_4 \tau_4 | \hat{O}_{12}^{(n)} \hat{O}_{34}^{(q)} | (\sigma_1 \tau_1, \sigma_2 \tau_2, \sigma_3 \tau_3, \sigma_4 \tau_4) \rangle_{\mathcal{P}} \quad (C5)$$

where only *linked* permutations are considered; for example, in the four-body term, the identical permutation $|\alpha_1 \beta_2 \gamma_3 \delta_4\rangle$ is not linked, because the only present links are between particles 12 and 34, but the two clusters are not connected; there are four unlinked permutations in this term.

[1] W. Glöckle *et al*, *Phys. Rep.* **274** (1996) 107.

[2] A. Kievsky, S. Rosati and M. Viviani, *Nucl. Phys.* **A551** (1993) 241 and *Private communication*

[3] H. Kamada et al., *Phys. Rev.* **C64**, (2001) 044001

[4] S. C. Pieper, R. B. Wiringa, *Ann. Rev. Nucl. Part. Sci.* **51**, 53 (2001)

[5] S.C. Pieper, R.B. Wiringa and V.R. Pandharipande, *Phys. Rev.* **C46**, 1741 (2000)

[6] I. Stetcu, B. R. Barrett, P. Navratil and J. P. Vary, *nucl-th/0412004*

[7] A. Fabrocini, F. Arias de Saavedra and G. Co', *Phys. Rev.* **C61**, (2000) 044302 and *Private Communication*;

[8] A. Fabrocini, F. Arias de Saavedra, G. Co' and P. Folgarait, *Phys. Rev.* **C57**, (1998) 1668

[9] G. Cò, *private communication*

[10] G. Co', A. M. Lallena, *Ann. Phys. (N.Y.)* **287**(2001)101

[11] S. R. Mokhtar, M. Anguiano, G. Co', A. M. Lallena, *Ann. Phys. (N.Y.)* **292**(2001)67

[12] C. Giusti and F. D. Pacati, *Nucl. Phys.* **A615** (1997)373

[13] S. Benhar and V. R. Pandharipande, *Phys. Rev.* **C47** (1993)2218
C. Ciofi degli Atti and S. Simula, *Phys. Lett.* **B325** (1994) 276

[14] C. Ciofi degli Atti and S. Liuti, *Nucl. Phys.* **A532**(1991)235

[15] By J. Ryckebusch, S. Janssen, W. Van Nespen, D. Debruyne, *Phys.Rev.* **C61**(2000)021603

[16] C. Barbieri, C. Giusti, F. D. Pacati, W. H. Dickoff, *Phys. Rev.* **C70** (2004) 014606

[17] *See, e.g.* L. L. Frankfurt, G. A. Miller and M. Strikman, *Ann. Rev. Nucl. Part. Sci.* **45** (1994) 501; N. N. Nikolaev, *Surv. High Energy Phys.* **7** (1994) 1

[18] S.J . Brodsky and A. H. Mueller, *Phys. Lett.* **B296** (1998) 685

[19] See e.g. B.Z. Kopeliovich, J. Nemchik, E. Predazzi and A. Hayashigaki, *Nucl. Phys.* **A740** (2004) 212

[20] C. Ciofi degli Atti, and D. Treleani, *Phys. Rev* **C60** (1999) 024602

[21] M. Alvioli, *PhD Thesis*, University of Perugia, 2004.

[22] M. Alvioli, C. Ciofi degli Atti and H. Morita, invited paper to the *2nd International Conference on Nuclear and Particle Physics with CEBAF at JLab*, Dubrovnik, Croatia, 2003 *Fizika B* **13** (2004) 585

- [23] H. Primakoff, T. Holstein, 1939, *Phys. Rev.* **55**, (1939) 1218
- [24] C.Ciofi degli Atti, in *Hadronic physics with multi-GeV electrons*, Les Houches Series, 1991
- [25] S. C. Pieper, R. B. Wiringa, *Ann. Rev. Nucl. Part. Scie.* **51** (2001) 53
- [26] J. W. Clark, *Progr. Part. Nucl. Phys.* **2**(1979)89
- [27] R. Guardiola, *Nucl. Phys.* **89 A**(1979) 328
- [28] R. Guardiola, M. Portesi, *J. Phys. G.* **24**(1998) L37
- [29] M. Gaudin, J. Gillespie and G. Ripka, *Nucl. Phys.* **A176** (1971) 237
- [30] O. Bohigas and S. Stringari, *Phys. Lett.* **95B** (1980) 9
- [31] M. Dal Rì and S. Stringari, *Nucl. Phys.* **A376** (1982) 81
- [32] O. Benhar, C. Ciofi degli Atti, S. Liuti and G. Salmè, *Phys. Lett.* **B177**, (1986) 135
- [33] O. Benhar and V. R. Pandharipande, *Rev. Mod. Physics* **65**(1993)817.
- [34] S.S. Dimitrova, D.N. Kadrev, A.N. Antonov and M.V. Stoitsov, *Eur. Phys. J.* **A7** (2000) 335
- [35] N.H. March, W.H. Young and S. Sampantar, *The many-body problem in quantum mechanics*, Cambridge 1967
- [36] R. B. Wiringa, V. G. J. Stoks, R. Schiavilla, *Phys. Rev.* **C51** (1995) 38
- [37] I. E. Lagaris and V. Pandharipande, *Nucl. Phys.* **A359** (1981) 331; **A359** (1981) 349
- [38] R.B. Wiringa, *Phys. Rev.* **C43**, (1991) 1585
- [39] L.R.B. Elton, *Nuclear size*, Oxford Univ.Press, London (1961)
- [40] H. De Vries, C. W. De Jager, C. De Vries, *Atom. Data and Nucl. Data Tables* **36**, (1987) 495
- [41] C. Ciofi degli Atti, S. Simula, *Phys. Rev.* **C53**, (1996) 1689.
- [42] M. Alvioli, C. Ciofi degli Atti, I. Marchino, H. Morita, *to appear*

TABLE I: The results of the benchmark calculation of the ground-state energy of ^{16}O using the $V8'$ interaction [36], the correlation functions shown in Fig. 1 [9], and harmonic oscillator mean field wave functions with parameter $a = 2 \text{ fm}$ (cf. Appendix A1). The results of the η -expansion obtained in this paper are compared with the FHNC/SOC results of Ref. [9]. $\langle V \rangle$ is the average potential energy, $\langle T \rangle$ the average kinetic energy, $E = \langle V \rangle + \langle T \rangle$ the total energy, and E/A the total energy per particle. The kinetic energy of the Center-of-Mass motion has been subtracted from the expectation value of the kinetic energy operator. All quantities in MeV .

approach	$\langle V \rangle$	$\langle T \rangle$	E	E/A
η -expansion, <i>this paper</i>	-390.37	323.50	-65.90	-4.12
<i>FHNC/SOC</i> , Ref. [9]	-390.30	325.18	-65.12	-4.07

TABLE II: The contributions $\langle V_i \rangle$ of the first six channels of the $V8'$ interaction to the average potential energy $\langle V \rangle$ shown in Table I. All quantities in MeV .

approach	$\langle V_c \rangle$	$\langle V_\sigma \rangle$	$\langle V_\tau \rangle$	$\langle V_{\sigma\tau} \rangle$	$\langle V_t \rangle$	$\langle V_{t\tau} \rangle$	$V = \sum_i V_i$
η -expansion, <i>this paper</i>	0.6	-35.4	-10.1	-172.8	-0.03	-172.7	-390.37
<i>FHNC/SOC</i> , Ref. [9]	0.7	-40.1	-10.6	-180.0	0.07	-160.3	-390.30

TABLE III: The results of the benchmark calculation of the ground-state energy of ^{40}Ca using the six-component truncated Urbana $U14$ interaction, the correlation functions shown in Fig. 2 [8], and harmonic oscillator mean field wave functions with HO parameter $a = 1.654$ fm(see Eq. (A2)). The results of the η -expansion obtained in this paper are compared with the FHNC/SOC results of Ref. [8]. Notations are the same as in Table I. All quantities in MeV .

approach	$\langle V \rangle$	$\langle T \rangle$	E	E/A
η expansion, <i>this paper</i>	-1655.15	1425.90	-229.25	-5.73
<i>FHNC/SOC</i> , Ref. [8]	-1891.60	1587.60	-314.80	-7.87

TABLE IV: The contributions of the first six channels of the $U14$ interaction to the average potential energy $\langle V \rangle$ shown in Table. III. Notations are the same as in Table I. All quantities in MeV .

approach	$\langle V_c \rangle$	$\langle V_\sigma \rangle$	$\langle V_\tau \rangle$	$\langle V_{\sigma\tau} \rangle$	$\langle V_t \rangle$	$\langle V_{t\tau} \rangle$	$V = \sum_i V_i$
η -expansion, <i>this paper</i>	-14.57	83.20	91.93	-1353.45	11.61	-473.87	-1655.15
<i>FHNC/SOC</i> , Ref. [8]	-8.40	92.00	108.40	-1549.20	11.60	-565.60	-1891.20

TABLE V: The results of the calculation of the ground-state energy and radius of ^{16}O using the full $V8'$ interaction, the correlation functions shown in Fig. 3 [7] and HO and SW mean field wave functions. The value of the HO parameter is $a = 2.0 \text{ fm}$ and the parameters of the SW well are as follows: $V_o = 42.0 \text{ fm}$, $R_o = 3.6 \text{ fm}$ and $a_o = 0.55 \text{ fm}$. The results of the η -expansion obtained in this paper are compared with the FHNC/SOC results of Ref. [7]. Notations are the same as Table I. $\langle r^2 \rangle$ is the rms radius. Energies in MeV , radii in fm .

Mean Field	Approach	$\langle V \rangle$	$\langle T \rangle$	E	E/A	$\langle r^2 \rangle^{1/2}$
HO	η -expansion, <i>this paper</i>	-420.39	350.39	-67.54	-4.40	2.99
HO	<i>FHNC/SOC</i> , Ref. [7]	-439.84	353.44	-86.40	-5.40	3.03

TABLE VI: The same as in Table V but for Woods-Saxon mean field wave functions.

Mean Field	Approach	$\langle V \rangle$	$\langle T \rangle$	E	E/A	$\langle r^2 \rangle^{1/2}$
SW	η -expansion, <i>this paper</i>	-500.59	444.10	-56.50	-3.50	2.64
SW	<i>FHNC/SOC</i> [7]	-519.68	428.16	-91.52	-5.72	2.83

TABLE VII: The same as in Table V, for ^{40}Ca ; the value of the HO parameter is $a = 2.1 \text{ fm}$.

Mean Field	Approach	$\langle V \rangle$	$\langle T \rangle$	E	E/A	$\langle r^2 \rangle^{1/2}$
HO	η -expansion, <i>this paper</i>	-1320.22	1048.22	-272.00	-6.80	3.72
HO	<i>FHNC/SOC</i> [7]	-1521.20	1193.60	-327.60	-8.19	3.65

TABLE VIII: The same as in Table VII but for the Woods-Saxon well with parameters $V_o = 50.0 \text{ fm}$, $R_o = 5.3 \text{ fm}$, $a_o = 0.53 \text{ fm}$.

Mean Field	Approach	$\langle V \rangle$	$\langle T \rangle$	E	E/A	$\langle r^2 \rangle^{1/2}$
SW	η -expansion, <i>this paper</i>	-1293.96	1018.19	-275.77	-7.00	3.75
SW	<i>FHNC/SOC</i> [7]	-1547.20	1215.20	-332.00	-8.3	3.66

TABLE IX: The values of the parameters appearing in the parametrization given by Eqs. B2a-B2b of the correlation functions of ^{16}O shown in Fig. 3.

n	$A_1^{(n)}$	$A_2^{(n)}$	$A_3^{(n)}$	$A_4^{(n)}$	$A_5^{(n)}$	$A_6^{(n)}$	$B_1^{(n)}$	$B_2^{(n)}$	$B_3^{(n)}$	$B_4^{(n)}$	$B_5^{(n)}$
1	1.0005	0.37314	-1.1781	0.	0.	0.	1.0	2.0	0.	0.	0.
2	0.	-0.1372	0.1916	-0.0226	-0.0141	0.	5.0	3.5	1.0	0.13	0.
3	0.	-0.0795	0.1271	-0.0121	-0.0330	0.	5.0	3.5	1.5	0.14	0.
4	0.	-0.3817	0.4863	-0.0535	-0.0424	0.	4.5	3.7	1.6	0.15	0.
5	0.	0.0114	0.0527	-0.0702	0.0064	0.	0.8	1.5	1.5	1.5	0.
6	0.	-0.1776	-0.0054	-0.0237	-0.00006	0.	1.7	1.0	1.3	0.01	0.

TABLE X: The same as in Table IX for the correlation functions of ^{40}Ca shown in Fig. 4.

n	$A_1^{(n)}$	$A_2^{(n)}$	$A_3^{(n)}$	$A_4^{(n)}$	$A_5^{(n)}$	$A_6^{(n)}$	$B_1^{(n)}$	$B_2^{(n)}$	$B_3^{(n)}$	$B_4^{(n)}$	$B_5^{(n)}$
1	1.00039	0.7576	-1.6015	0.	0.	0.	3.9	2.9	0.	0.	0.
2	0.	-0.0573	0.0965	-0.0156	-0.0145	0.	7.0	3.5	0.8	0.2	0.
3	0.	-0.0207	0.0474	-0.0019	-0.0279	0.	8.5	3.5	2.0	0.215	0.
4	0.	-0.0290	0.0906	-0.0237	-0.0356	0.	9.4	3.0	1.0	0.22	0.
5	0.	0.0165	0.0061	0.0009	-0.0188	-0.0041	1.0	3.0	0.3	1.3	4.5
6	0.	-0.1342	0.00013	-0.0368	0.00044	-0.00069	1.55	0.02	1.4	0.1	0.1

TABLE XI: The value of $C_D^{(p,q)}(\mathbf{r}_{12}, \mathbf{r}_{1'2})$ and $C_E^{(p,q)}(\mathbf{r}_{12}, \mathbf{r}_{1'2})$ defined in Appendix C. The order of the operator $p, q = 1, 2, \dots, 6$ is the same as Table II. Here $\langle S_{12}S_{1'2} \rangle$ is defined as $\langle S_{12}S_{1'2} \rangle = 12(3(\hat{\mathbf{r}}_{12} \cdot \hat{\mathbf{r}}_{1'2})^2 - 1)$, with the definition of $\hat{\mathbf{r}} = \mathbf{r}/r$.

Operator						
p/q	1	2	3	4	5	6
1 D	16	0	0	0	0	0
	E	4	12	12	36	0
2 D		48	0	0	0	0
	E	-12	36	-36	0	0
3 D			48	0	0	0
	E		-12	-36	0	0
4 D				144	0	0
	E			36	0	0
5 D					$4\langle S_{12}S_{1'2} \rangle$	0
	E				$2\langle S_{12}S_{1'2} \rangle$	$6\langle S_{12}S_{1'2} \rangle$
6 D						$12\langle S_{12}S_{1'2} \rangle$
	E					$-6\langle S_{12}S_{1'2} \rangle$

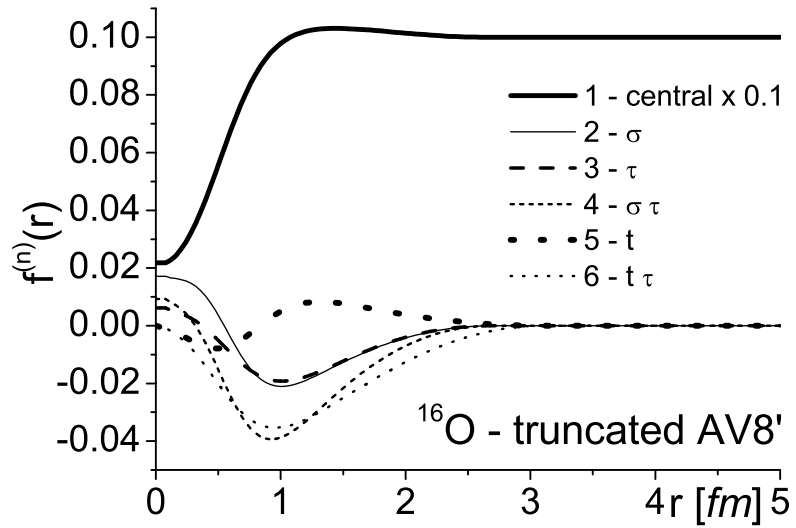


FIG. 1: The correlation functions for ^{16}O corresponding to the truncated Argonne $AV8'$ interaction [36] used in the benchmark calculation (After Ref. [9]).

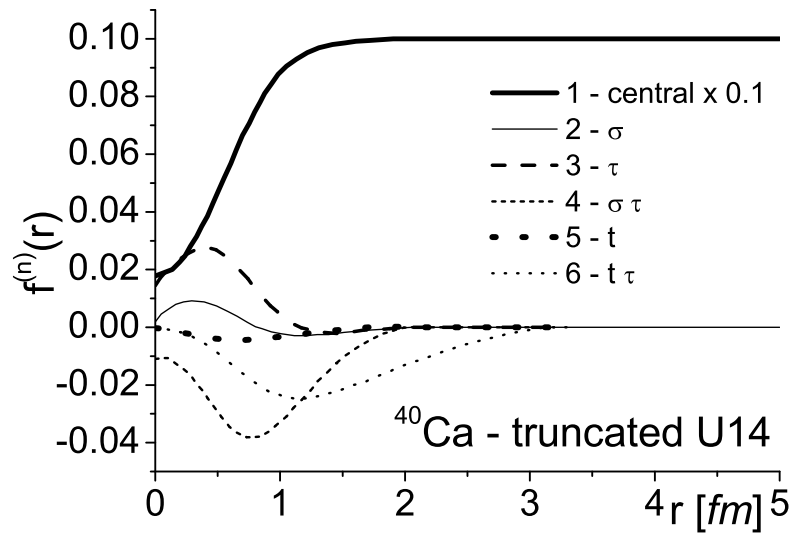


FIG. 2: The correlation functions for ^{40}Ca corresponding to the truncated Urbana $U14$ interaction [37] used in the benchmark calculation [36] (After Ref. [9]).

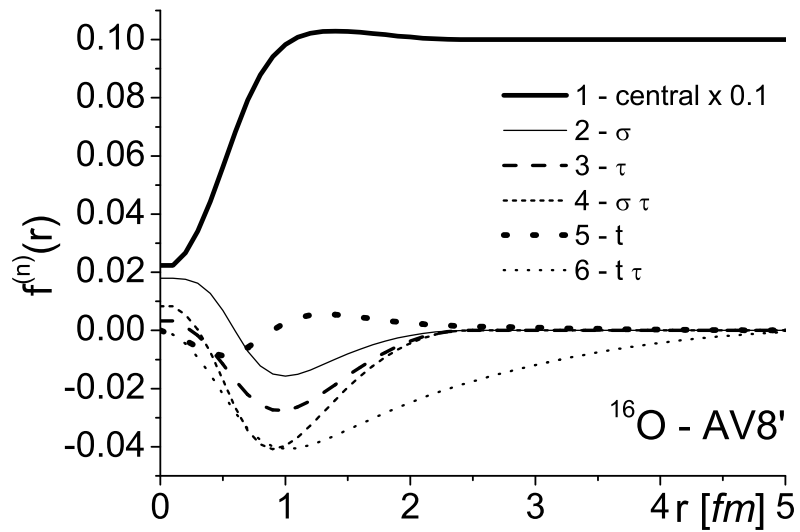


FIG. 3: The correlation functions for ^{16}O corresponding to the $AV8'$ interaction (After Ref. [7]).

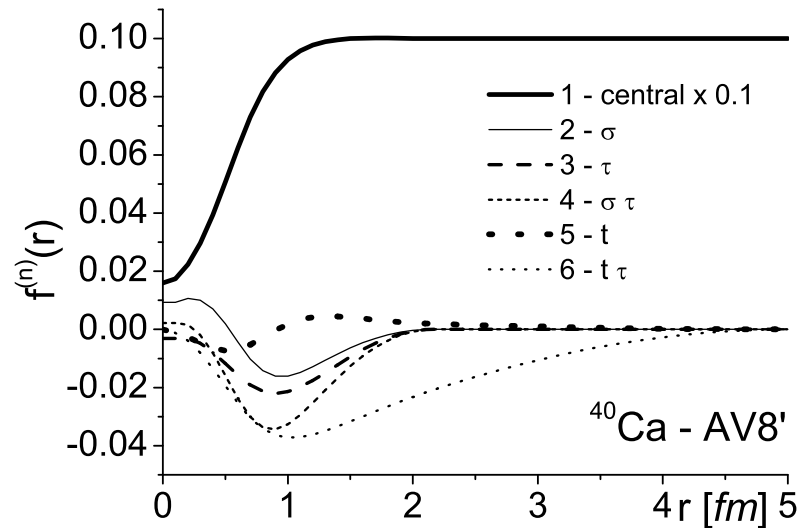


FIG. 4: The correlation functions for ^{40}Ca from [7], corresponding to the $AV8'$ interaction [36] (After Ref. [7]).

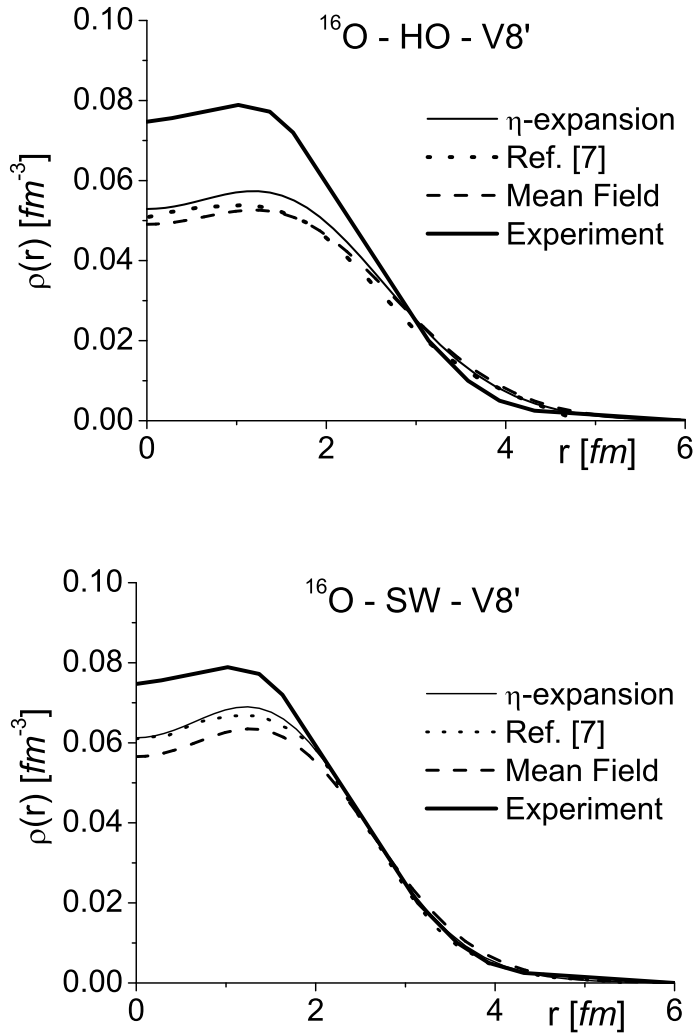


FIG. 5: The charge density of ^{16}O . *Thick full*: experimental density. *Thin full*: results of the η -expansion with harmonic oscillator (HO, *top*) and Saxon-Woods (SW, *bottom*) wave functions and correlations functions shown in Fig. 3. The wave function parameters correspond to the minimization of the ground-state energy. *Dots*: mean field density obtained by setting $f^{(1)} = 1$, $f^{(n \neq 1)} = 0$. The charge density is obtained by folding the matter density with the charge density of the proton and correcting for the center-of-mass motion effects. The value of the rms radius is $\langle r^2 \rangle^{1/2} = 3.07 \text{ fm}$, with HO wave functions, and $\langle r^2 \rangle^{1/2} = 2.85 \text{ fm}$, with SW wave functions. The value of the HO parameter is $a = 2.00 \text{ fm}$ and the parameters of the SW well are $V_o = 42.0 \text{ fm}$, $R_o = 3.6 \text{ fm}$ and $a_o = 0.55 \text{ fm}$. The density normalization is $\int d\mathbf{r} \rho(r) = Z$.

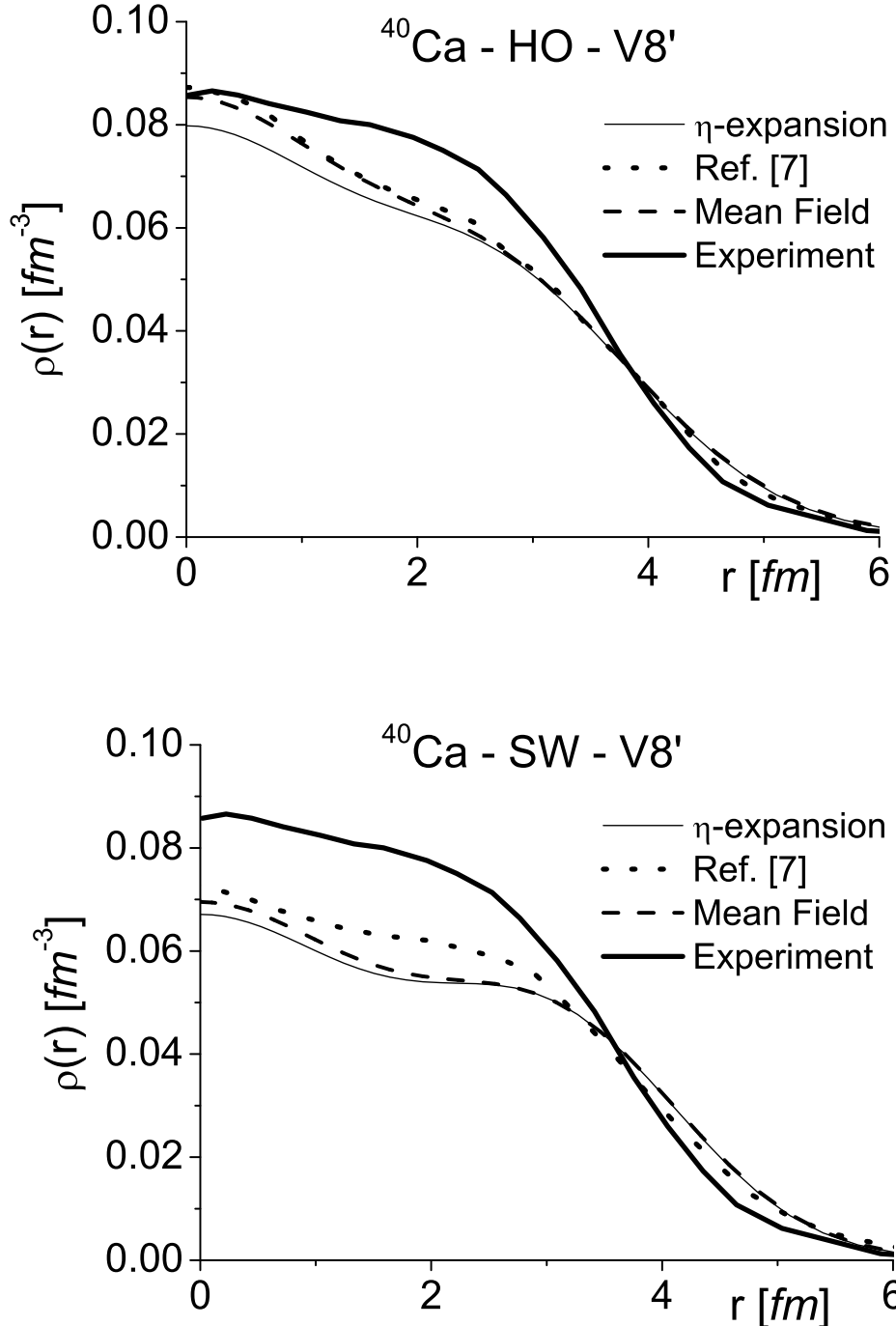


FIG. 6: The same as in Fig. 5, but for ^{40}Ca , and correlation functions from Fig. 4. The value of the rms radius is $\langle r^2 \rangle^{1/2} = 3.72 \text{ fm}$, with HO wave functions, and $\langle r^2 \rangle^{1/2} = 3.75 \text{ fm}$, with SW wave functions; the value of the HO parameter is $a = 2.10 \text{ fm}$, and the parameters of the SW well are $V_o = 50.0 \text{ fm}$, $R_o = 5.3 \text{ fm}$ and $a_o = 0.53 \text{ fm}$.

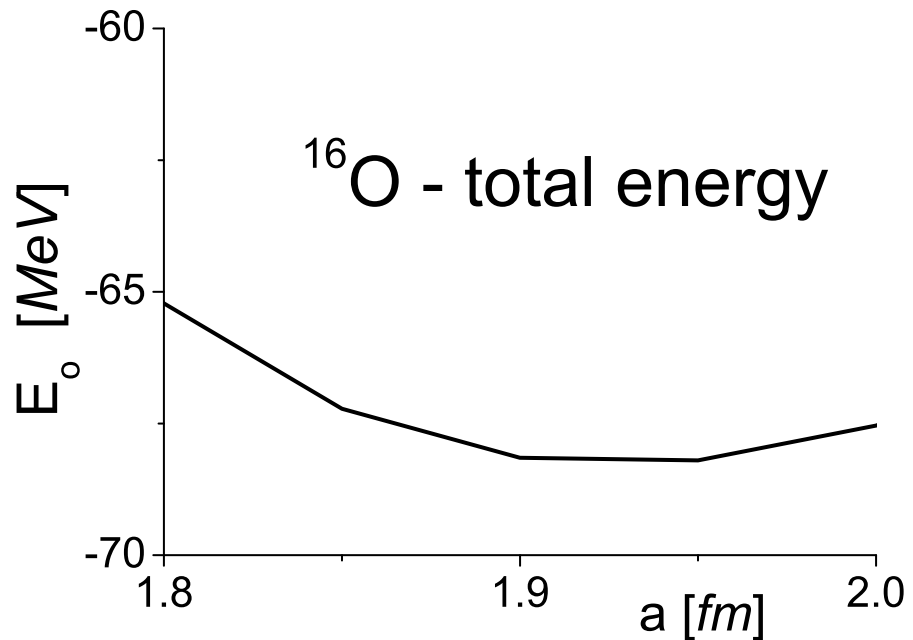


FIG. 7: The ground-state energy of ^{16}O versus the harmonic oscillator parameter a calculated with the η -expansion and the $V8'$ interaction, using the correlation functions shown in Fig.3.

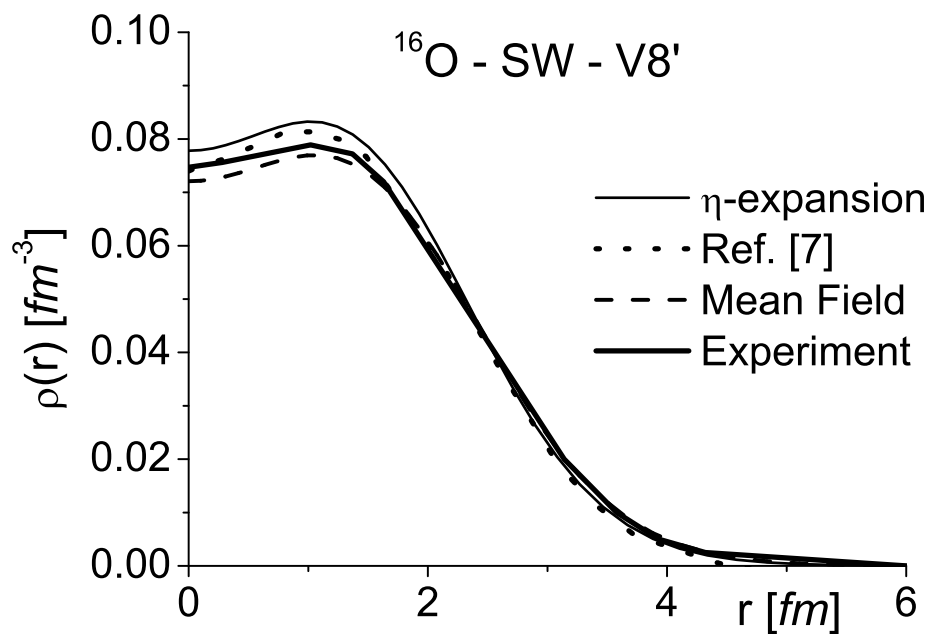
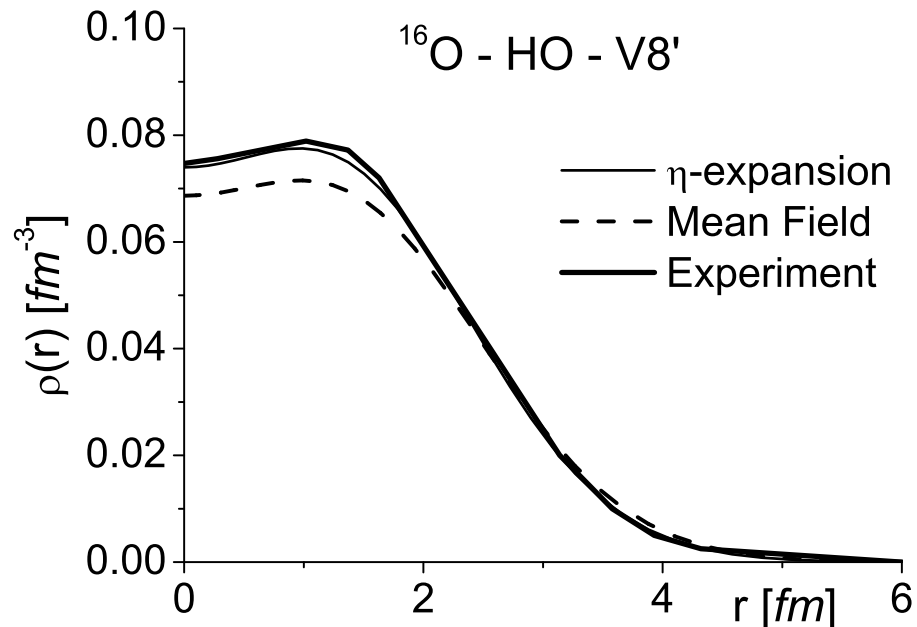


FIG. 8: The same as in Fig. 5, but with mean field wave functions chosen so as to better reproduce the experimental density. The value of the rms radius is $\langle r^2 \rangle^{1/2} = 2.73$ fm, with HO wave functions, and $\langle r^2 \rangle^{1/2} = 2.71$ fm, with SW wave functions. The value of the HO parameter is $a = 1.81$ fm, and the parameters of the SW well are $V_o = 53.0$ fm, $R_o = 3.45$ fm and $a_o = 0.7$ fm.

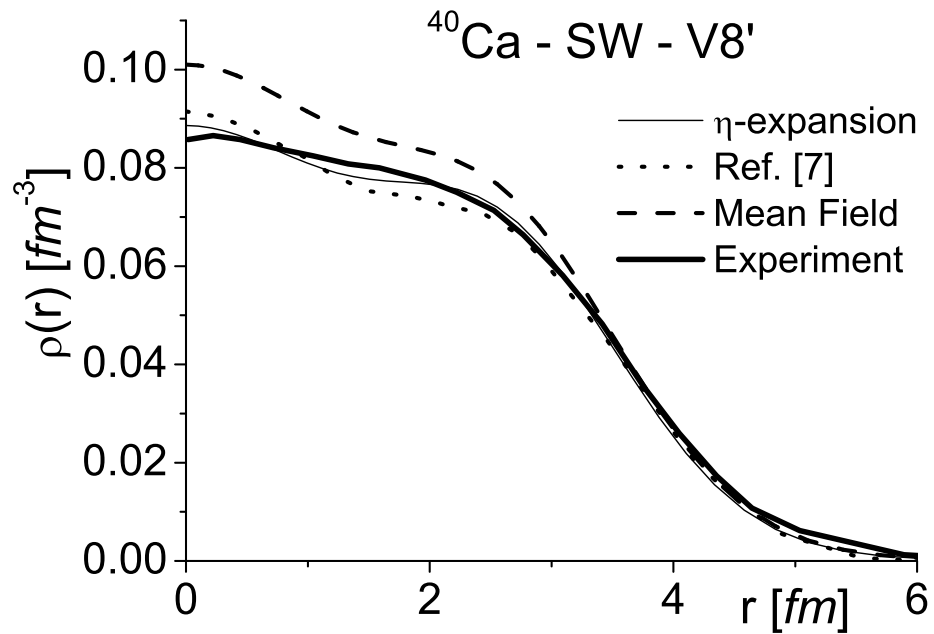
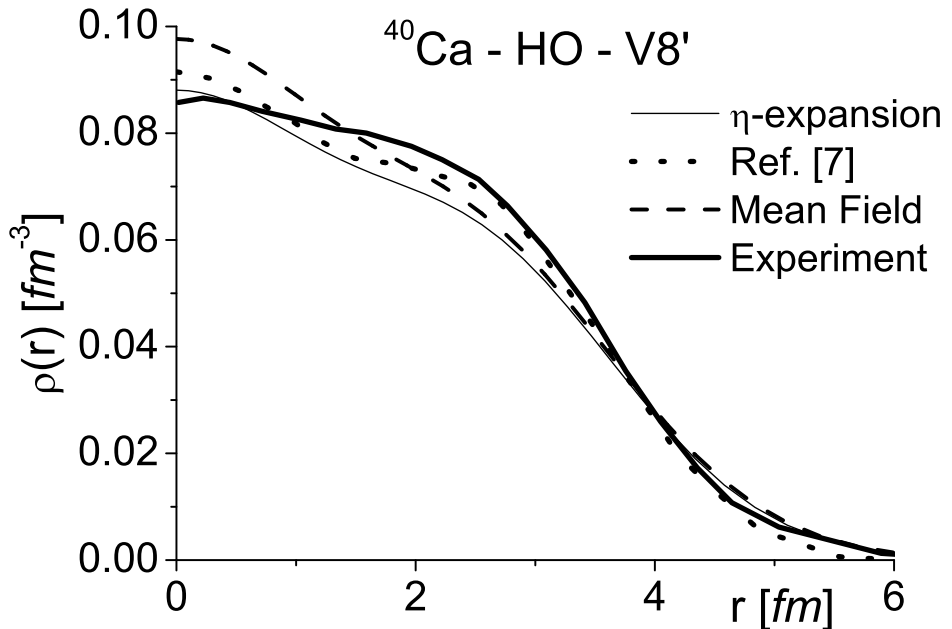


FIG. 9: The same as in Fig. 6, but for ^{40}Ca . The value of the rms radius is $\langle r^2 \rangle^{1/2} = 3.56 \text{ fm}$, with HO wave functions, and $\langle r^2 \rangle^{1/2} = 3.34 \text{ fm}$, with SW wave functions. The value of the HO parameter is $a = 2.00 \text{ fm}$ and the parameters of the SW well are $V_o = 50.0 \text{ fm}$, $R_o = 5. \text{ fm}$ and $a_o = 0.515 \text{ fm}$.

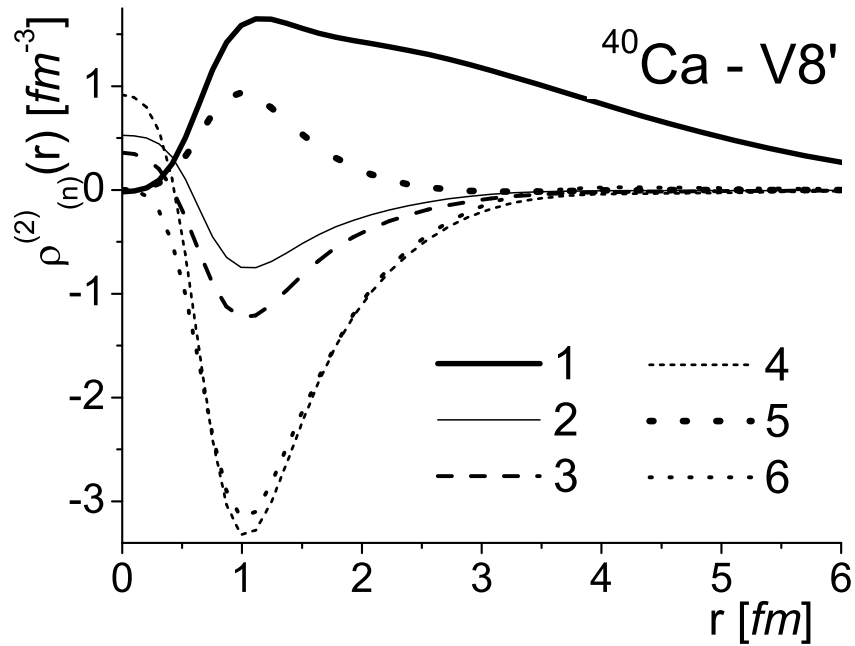
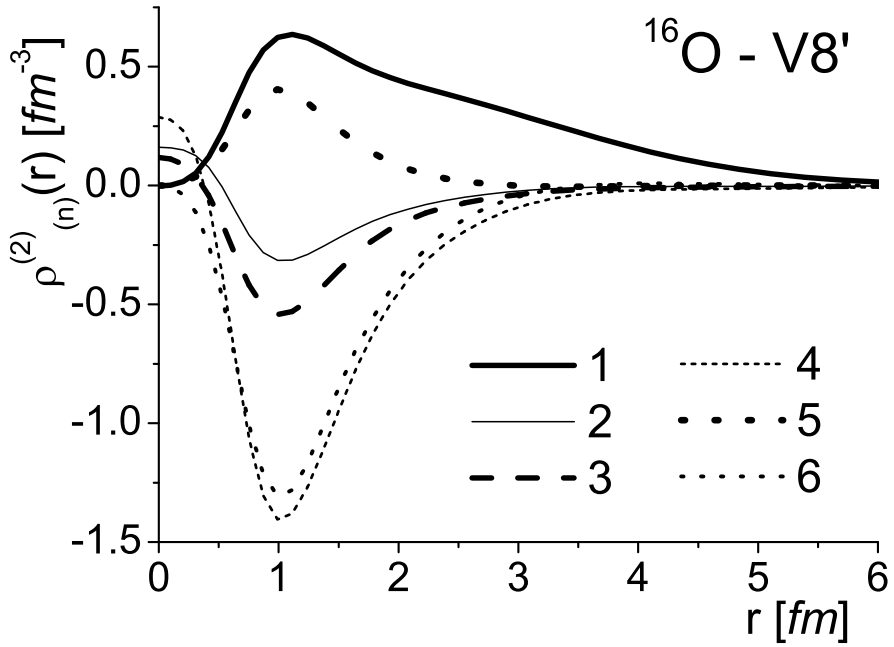


FIG. 10: The two-body densities (Eq. (42)) of ^{16}O and ^{40}Ca corresponding to the correlation functions of Fig. 3 (^{16}O) and Fig. 4 (^{40}Ca); the quantities in the figure are integrated over the center of mass coordinate (see Eq. (51)). The splitting of the two-body density in n different quantities is explained in Eq. (42) and the following text.

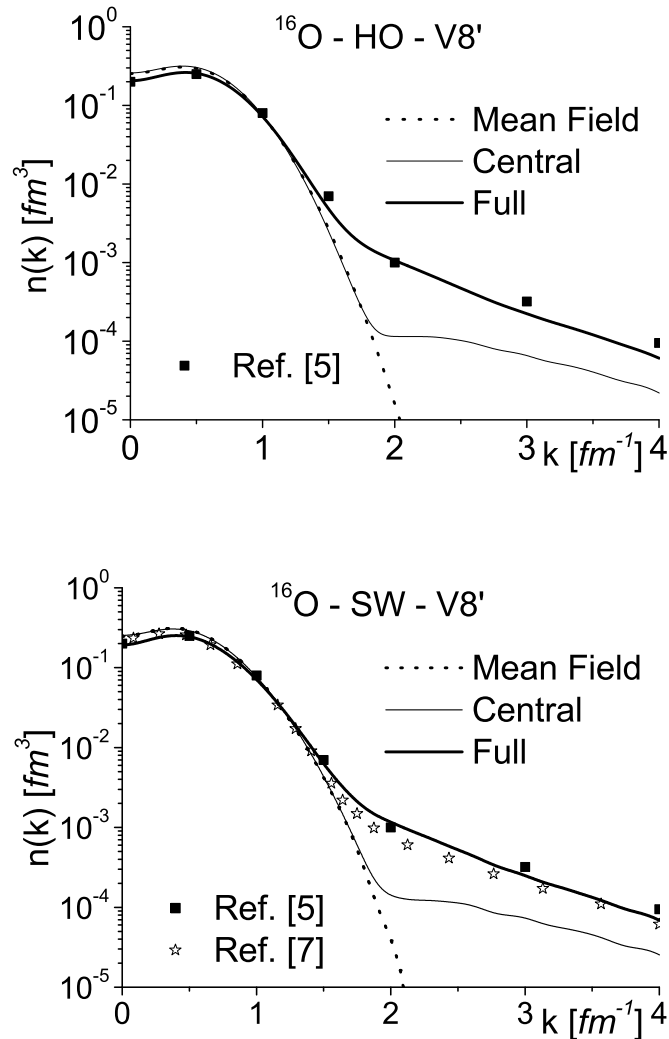


FIG. 11: The momentum distributions of ^{16}O corresponding to harmonic oscillator (*top*) and Saxon-Woods (*bottom*) wave functions giving the best density shown in Fig. 8. The full thin line includes only the central correlation function, whereas the thick full line includes all of them. Our results are compared with the results of Ref. [7] (*stars*), obtained with the same correlation functions. The results of Ref. [5] obtained within the VMC approach using the AV14 interaction are also shown by full squares. The value of the kinetic energy obtained by integrating $n(k)$ are: $\langle T \rangle = 297.87$ (*central, HO*), $\langle T \rangle = 476.55$ *MeV* (*full, HO*); $\langle T \rangle = 306.99$ (*central, SW*) and $\langle T \rangle = 494.48$ *MeV* (*full, WS*). The normalization of $n(k)$ is $\int d\mathbf{k} n(k) = 1$.

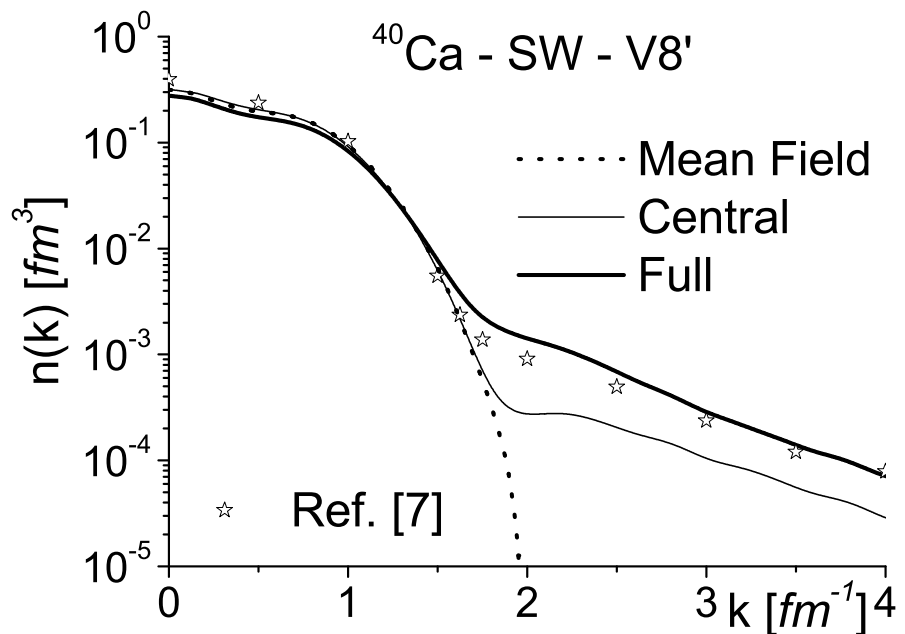
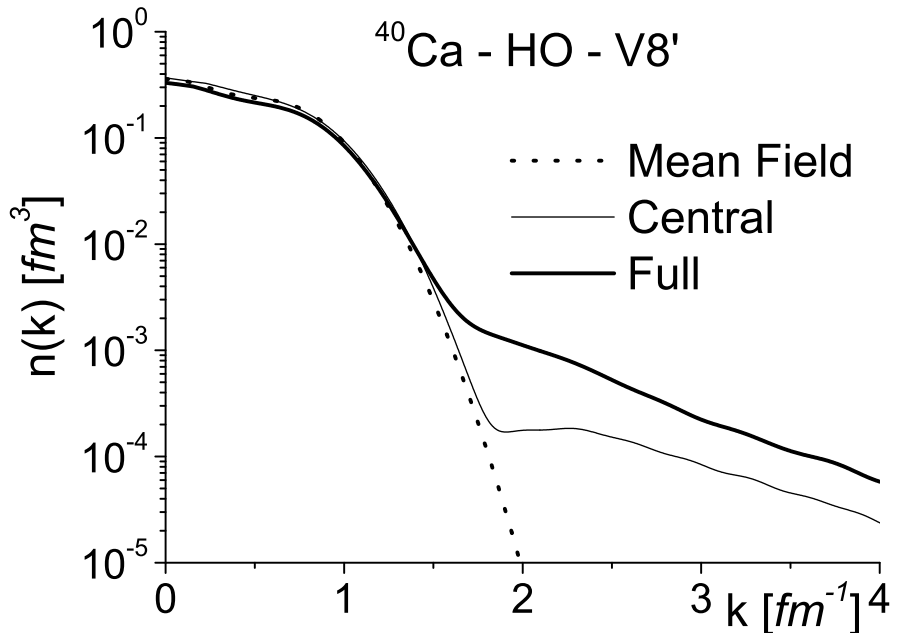


FIG. 12: The same as in Fig. 11, but for ^{40}Ca and correlation functions from Fig. 4 and mean field wave functions giving the best charge density of Fig. 9. The value of the kinetic energy obtained by integrating $n(k)$ are $\langle T \rangle = 782.87$ (central, HO), $\langle T \rangle = 1178.45$ MeV (full, HO); $\langle T \rangle = 836.24$ (central, SW) and $\langle T \rangle = 1245.21$ MeV (full, SW).

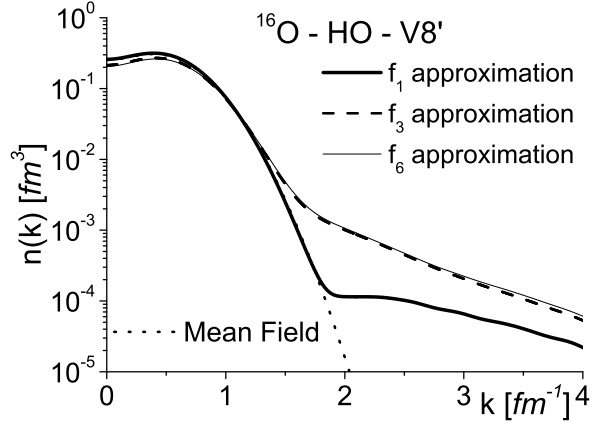


FIG. 13: The effect of the various correlation functions on the momentum distribution of ^{16}O . f_1 approximation: only central correlation; f_3 approximation: $f^{(2)} = f^{(3)} = f^{(5)} = 0$. f_6 approximation: full correlation set, $n = 1, \dots, 6$. Calculations were performed with correlation functions taken from Fig. 3 and HO wave functions.

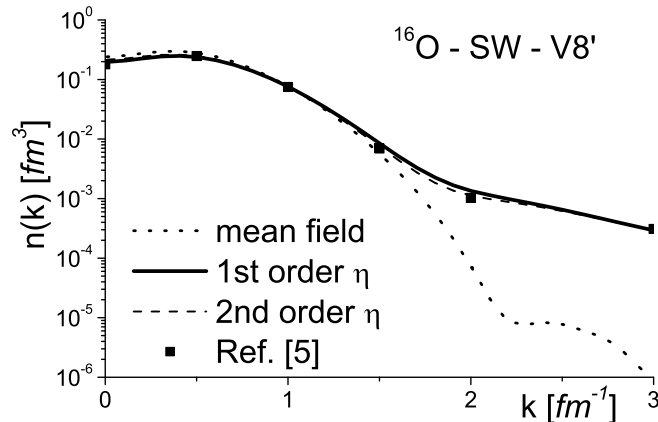


FIG. 14: The convergence of the momentum distributions of ^{16}O calculated by considering the 1st and 2nd orders of the η -expansion, Saxon-Woods mean field wave functions, the f_3 approximation and the correlation functions of Fig. 3. Our results are compared with the results of Ref. [5] obtained within the VMC approach and the AV14 interaction. The values of the kinetic energies obtained by integrating the momentum distributions are: $\langle T \rangle = 521.87$ MeV (mean field), $\langle T \rangle = 980.10$ MeV (1st order η), $\langle T \rangle = 932.64$ MeV (2nd order η). The normalization of $n(k)$ is $\int dk n(k) = 1$.

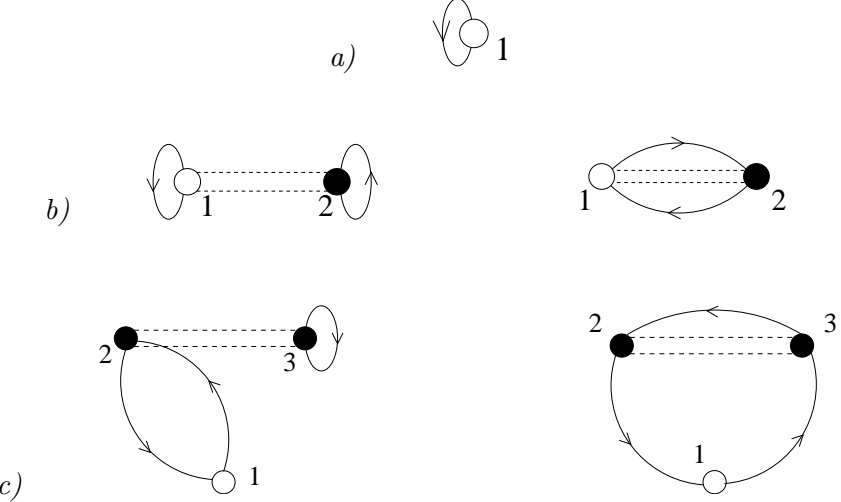


FIG. 15: Diagrammatic representation of the one body density $\rho(\mathbf{r}_1)$ in the lowest order of the η -expansion (Eq. (50)). Dots denote the corresponding spatial coordinates and integrations occur over full dots. An oriented full line represents the shell model uncorrelated non diagonal density matrix $\rho_o^{(1)}(i, j)$, an oriented closed line the diagonal density matrix $\rho_o(i, i)$, and a dotted line the correlation $H(r_{ij}, r_{ji})$ between particles i and j . *a*): shell model, uncorrelated density ρ_o ; *b*): hole contribution $\Delta\rho^H$ *c*): spectator contributions $\Delta\rho^S$. The direct and exchange contributions are shown on the left and right sides of the Figure, respectively.

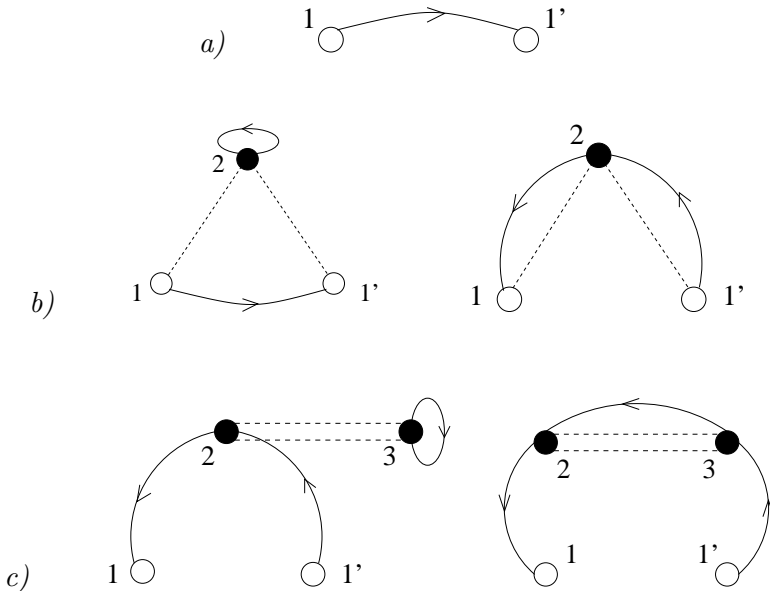


FIG. 16: The same as in Fig. 15 for the one body mixed density matrix $\rho^{(1)}(\mathbf{r}, \mathbf{r}')$.

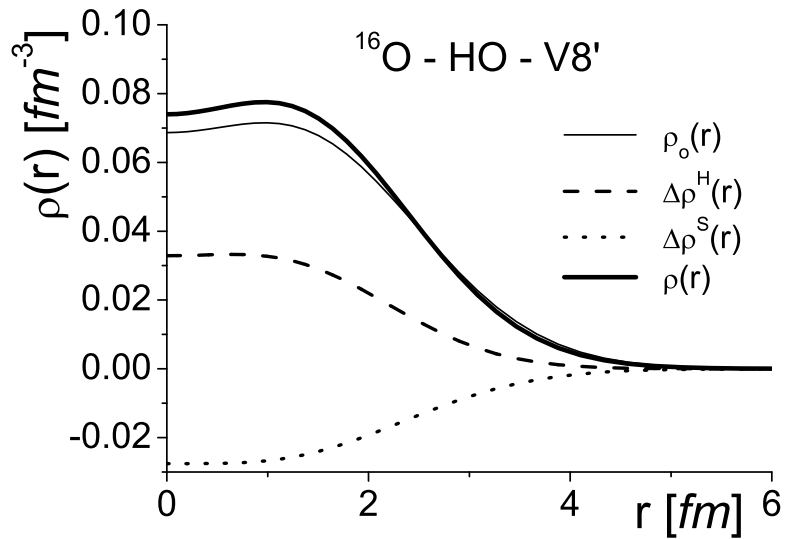


FIG. 17: The charge density of ^{16}O . *Thin full*: shell model density (Eq. (33)). *Thick full*: correlated density (Eq. (50)) calculated with the correlation functions of Fig. 3 [7] and HO mean field Wave Functions with parameter $a = 1.8 \text{ fm}$. *Dashed*: hole contribution $\Delta\rho^H(r)$; *dotted*: spectator contribution $\Delta\rho^S(r)$.

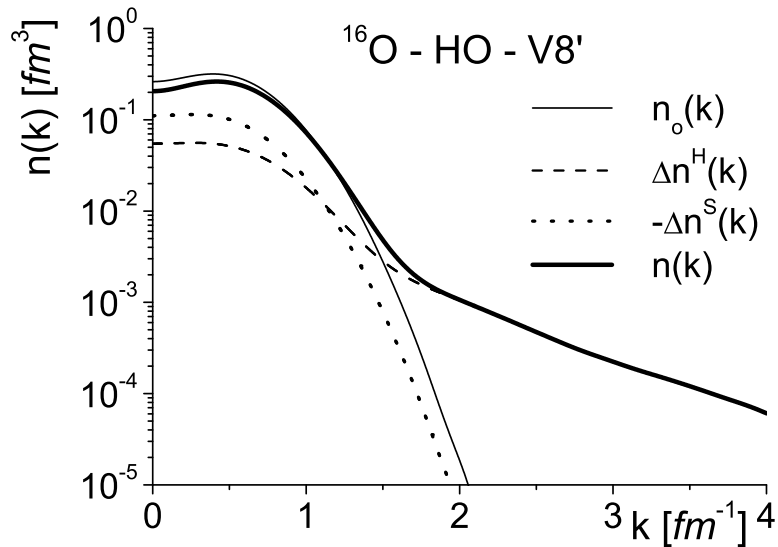


FIG. 18: The same as in Fig. 17, but for the momentum distribution.